



Sudan University of Sciences and Technology
College of Graduate Studies

**Evaluation of Entrance Skin Radiation Exposure Dose
for Pediatrics Examined by Digital Radiography**

تقويم الجرعة الداخلة للجلد لدى الأطفال الذين تم تصويرهم بالأشعة الرقمية

A Thesis submitted for Fulfillment for the Degree
(M. Sc) in Diagnostic Radiologic Technology

By

Sami Nasreldeen Abdelwally Eljak

Supervisor

Dr .Caroline Edward Ayad Khela
Associate professor
(July 2015)

الآية الكريمة



(الَّذِينَ آمَنُوا وَتَطْمَئِنُّ قُلُوبُهُمْ بِذِكْرِ اللَّهِ أَلَا بِذِكْرِ اللَّهِ تَطْمَئِنُّ الْقُلُوبُ)

{الرعد: 28}

صدق الله العظيم

DEDICATION

I dedicate this research to my:

Parents...

Family ...

Friends ...

ACKNOWLEDGMENT

First of all, I thank Allah the Almighty for helping me complete this research. I thank Dr. Caroline Edward Ayad Khela, my supervisor, for her help and guidance.

I would like to express my gratitude to Dr. Ragab Hani, Dr. Yousif Mohamed Yousif and the whole staff of the radiological unit in Aseer Central Hospital for their great help and support.

Finally I would like to thank everybody who helped me prepare and finish this study.

ABSTRACT

The main objective of this study to evaluate the entrance skin radiation exposure dose for pediatrics that examined by digital radiography because the Entrance skin dose (ESD) of pediatric x-ray department may be exceeding the reference dose level and many departments don't use recommended radiographic parameters for pediatrics. measured the entrance skin dose (ESD) received by 152 pediatrics (78 males and 74 females) aged between 2- 15 years old undergoing 12 types of diagnostic X-ray examination at Radiology Department of Asser Central Hospital-KSA in period between august 2013 to July 2015.

The entrance skin dose ESD was determined via measurements parameters: focus to skin distance (FSD), tube current (mAs)and tube voltage (kV) in arithmetical equation .The mean \pm SD for ESDs were found to be 0.16 ± 0.03 , 0.21 ± 0.01 , 0.63 ± 0.26 , 0.58 ± 0.09 , 0.20 ± 0.05 , 0.26 ± 0.06 , 0.44 ± 0.19 , 0.46 ± 0.18 , 0.52 ± 0.12 , 0.21 ± 0.02 , 0.35 ± 0.01 , 0.28 ± 0.03 , for PA chest, foot, AP pelvis, PA skull, PA hand, AP arm, ankle, AP shoulder, abdomen, forearm, AP femur, AP elbow consequently.

The mean ESD values obtained are found to be within the standard reference. The data obtained may add to the available information in national records for general use. It may provide guidance on where efforts on dose reduction will need to be directed to fulfill the requirements of the optimization process and serve as a reference for future researches.

ملخص البحث

الهدف الأساسي من هذه الدراسة هو تقييم الجرعة الإشعاعية الداخل للجلد للأطفال في التصوير الرقمي وذلك لان الجرعة الإشعاعية الداخل للجلد للأطفال في أقسام الأشعة قد تكون أكبر من مستوى الجرعة المرجعية كما أن بعض الأقسام لا تستخدم عوامل التعريض الموصى بها للأطفال.

تم قياس الجرعة الإشعاعية لعدد 152 طفل (78 ذكر ، 74 أنثى) أعمارهم بين (2-15 سنة) لعدد 12 فحص أجريت بمستشفى عسير المركزي بأبها –المملكة العربية السعودية في الفترة بين أغسطس 2013 إلى يوليو 2015.

الجرعة الإشعاعية للجلد تم تحديدها بقياس المتغيرات التالية (المسافة بين بؤرة أنبوب الأشعة و سطح المريض، فرق الجهد المطبق في أنبوب الأشعة، التيار المستخدم بالإضافة لزمان التعريض وتطبيق المتغيرات في معادلة رياضية. متوسط الانحراف المعياري للجرعة التي تعرض لها الجلد كالتالي:

0.06 ± 0.26 ، 0.05 ± 0.20 ، 0.09 ± 0.58 ، 0.26 ± 0.63 ، 0.01 ± 0.21 ، 0.03 ± 0.16 ،
 0.03 ± 0.28 ، 0.53 ± 0.35 ، 0.02 ± 0.21 ، 0.12 ± 0.52 ، 0.18 ± 0.46 ، 0.19 ± 0.44
للأوضاع التالية: (الخلفي الأمامي للصدر، القدم، الأمامي الخلفي للحوض، الخلفي الأمامي للرأس، الخلفي الأمامي لليد، الأمامي الخلفي للعضد، الكاحل، الأمامي الخلفي للكتف، البطن، الساعد، الفخذ، الأمامي الخلفي للمرفق علي التوالي).

وجد أن متوسط الجرعة الداخلة للجلد تقع ضمن القيمة المرجعية البيانات التي تم جمعها يمكن اعتمادها كبيانات للاستخدام العام واعتبارها دليل يضاف للجهود التي تبذل لتقليل الجرعات الإشعاعية واعتبارها كقيم مرجعية لأي بحوث مستقبلية.

List of abbreviations

Abbreviation	Phrase
ALARA	As low as reasonably achievable
ESD	Entrance skin dose
KVP	Kilovoltage peak
mAs	Milliamperere second
HVL	Half value layer
Mev	Mega electron volte
ICRP	International Commission On radiation protection
EUCD	European Union Council Directive
IAEA	International Atomic Energy Agency
TLD	Thermo luminescence dosimeter
TIC	Transmission Ionizing Chamber
SSD	Surface skin distance
QC	Quality control
SID	Source to image distance
FSD	Focus to Image Distance
FFD	Focus to film distance
NRPB	National radiation protection board
CCD	Charge couple device
DR	Digital radiography
TFT	Thin- film transistor
DSA	Digital system angiogram
NSR	Signal-to noise ratio
DQE	Detective quantum efficiency
CR	Computed tomography
SF	Screen film
PACS	Picture archiving and communication system
AEC	Automatic exposure control

List of figures

Figure No	Title	Page
2-1	William C. Roentgen photograph	4
2-2	Roentgen's wife hand radiograph	5
2-3	The photon as the wave diagram	6
2-4	The photon as the particle diagram	6
2-5	Excitation process diagram	8
2-6	Ionization process diagram	9
2-7	Bremstrahlung process diagram	10
2-8	X-ray spectrum diagram	11
2-9	Effect of Tube current on X-ray spectrum diagram	12
2-10	Effect of Tube potential on X-ray spectrum diagram	13
2-11	Effect of filtration on X-ray spectrum diagram	14
2-12	Effect of atomic number on X-ray spectrum diagram	15
2-13	Effect Schematic diagram of classical scattering diagram	16
2-14	Schematic diagram of Compton scattering diagram	17
2-15	Schematic diagram of photoelectric effect diagram	19
2-16	Schematic diagram of pair production diagram	20
2-17	Schematic diagram of photodisintegration diagram	21
2-18	The photon absorption fractions diagram	25
2-19	Indirect capture DR system diagram	35
2-20	Direct capture DR system diagram	36
2-21	Conventional radiography latent image formation	37
2-22	CR latent image formation	38
3-1	Digital radiography photograph	47

List of tables

Table No	Title	Page
4-1	The mean and \pm SD values of all the pediatrics examined in the study	50
4-2	Mean and standard deviation for ESDs in mGy for the radiological examinations (projections)	50
4-3	Mean and standard deviation for ESDs in mGy for the radiological examinations (part under examination)	51
4-4	Mean and standard deviation for ESDs in mGy for the radiological examinations (Age class)	51
4-5	Mean and standard deviation for ESDs in mGy for the radiological examinations (gender)	52
4-6	Pearson Correlation (Weight, BMI and Height)	52
4-7	Pearson Correlation (Tube Voltage (KV), MAS, Organ thickness and Distance (FSD))	53

Tables of Contents

Topic	Page number
الآية الكريمة	I
Dedication	II
Acknowledgement	III
English Abstract	IV
Arabic Abstract	V
List of abbreviations	VI
List of figures	VII
List of tables	VIII
Table of contents	IX
Chapter One	
1- Introduction	1
1-1 Problem of the study	2
1-2 Objectives	2
1-3 Significance of the study	2
1-4 Overview of study	2
Chapter Two	
2.Theoretical Background	4
2-1 Theory of X-ray production	7
2-1-1Excitation	8
2-1-2 ionization	8
2-1-3 Bremsstrahlung	9
2-2 X-ray spectrum and beam characteristics	10
2-2-1 X-ray spectrum	10
2-2-2 X -ray beam characteristics	11
2.2.2.1 X -ray beam quantity	11
2.3 X-ray beam quality	15
2. 4. Interaction of radiation with matter	16
2-4-1 Coherent Scattering	16
2-4-2 Compton scattering	17
2-4-3 Photoelectric absorption	19
2-4-5 Pair production	20
2-2-6 Photodisintegration	21
2.5 Digital radiography	22

2.6 Advantages and Limitations of DR	23
2.7 Factors affecting image quality	24
2.8 Detection Efficiency	24
2.9 Dose creep in digital radiography and its prevention	26
2.9 Exposure indicators for digital radiography	27
2.10 Pediatric imaging issues	28
2.11 Proper exposure factors for standard examinations	30
2.12 Automatic exposure control	33
2.13 Indirect capture	35
2.14 Direct capture	35
2.15 Comparison of CR and DR with Conventional Radiography	36
2.16 previous studies	40
2.17 Calculation methods of entrance skin dose	43
Chapter Three	
3 Materials	46
3.1 Population of the study	46
3.2 Study sample	46
3.3 Inclusion criteria	46
3.4 Exclusion criteria	46
3.5 Ethical consideration	46
3.6 Data analysis	47
3.7 The machine used	47
3.8 Methods	48
3.8.1 X-ray technique used	48
3.8.2 Measure of the entrance skin dose	48
3.8.3 Data collection	49
Chapter Four	
4 Results	50

Chapter Five	
5 Discussion	54
5-1 Conclusion	57
5-2 Recommendation	58
References	59

CHAPTER ONE

1. Introduction

Assessment of radiation exposure during X-ray examinations are of great importance in radiation protection field. Pediatrics radiology should be governed with high professional's techniques to minimize radiation hazard on children while they are examined by X-ray. The parameters which involved in this project are ,X-ray tube voltage, X-ray tube current and the distance between the X-ray tube and patient's skin (child).Different radiographic examinations representing different radiographic techniques (tube voltage and current)were recorded reflecting the variety in the radiation exposure value. Also there is an increasing interest in investigating the methods to reduce the dose received by the pediatric due to medical exposure, in line with the directives of Health Protection laws. For diagnostic radiological examinations the basic concept is optimization, in order to use the minimum necessary dose to achieve a good image quality. (ICRP Publication 73 1996), Radiography of pediatric patients poses specific challenges: On one hand these anatomies show only little intrinsic contrast because of the still immature bone development. On the other hand children are more sensitive to radiation than adults because of the more rapidly dividing cells and the longer life expectancy. Optimization of x-ray imaging parameters must be guided by the ALARA principle (as low as reasonably achievable) (Willis, et al., 2004).

That means that the dose to the patient should be at the lowest level that still guarantees a sufficient diagnostic image quality.

1.1 Problem of the study:

The Entrance skin dose (ESD) of pediatric x-ray department may be exceeding the reference dose level. And many departments don't use recommended radiographic parameters for pediatrics also Poor collimation of the beam during examination may lead to irradiate unnecessary organs.

1.2 Objective of the study: To evaluate entrance skin radiation exposure dose for pediatric cases that examined by digital radiography.

1.3 Significance of the study:

Radiation dose to patients and its management have become important considerations in digital radiographic imaging procedures, but they acquire particular significance in the imaging of children. Because of their longer life expectancy, children exposed to radiation are thought to have a significantly increased risk of radiation-related late sequel compared to adults first exposed to radiation later in life. Therefore, current clinical thinking dictates that dose in pediatric radiography be minimized, while simultaneously ensuring sufficient diagnostic information in the image, and reducing the need for repeat exposures (Cohen 2002).

1.4 Overview of the study:

This prospective study was performed in the period of August 2013 to July 2015. Patients were examined at the radiology department of Asser Central Hospital-Saudi Arabia. Prior to patients examined, a formal approval was obtained from the Ethics and Scientific Committee of this medical center.

Informed consents were obtained from patients. This study consisted of five chapters. Chapter one is an introduction which include: problem, objective of the study, significance of the study and overview of the study. Chapter two is theoretical background, literature review and previous studies. Chapter three is material and methods. Chapter four is results Chapter five is discussion, conclusions and recommendations.

CHAPTER TWO

2. Theoretical Background:

The X-rays were accidentally discovered in 1895, when William C. Roentgen (Figure 2.1) was experimenting with a cathode ray tube.



Figure 2.1: William C. Roentgen . (ar-encyclopedia.blogspot, 2010)

Roentgen was working in his laboratory at Würzburg University in Germany. He had darkened his laboratory and completely enclosed his tube with a black paper so that he could better visualize the effects of the cathode rays in the tube (Curry 1984). A plate coated with barium platinocyanide (a fluorescent material) happened to be laying on a bench top several feet from the tube he was using. No visible light escaped from his tube because of the black paper enclosing the tube, but Roentgen noted that the barium platinocyanide fluoresced regardless of its distance from the tube (Curry 1984). Because the cathode rays Roentgen was studying could not travel more than a few centimeters in air, he concluded that the source of that glow of the plate he

noted was another kind of unknown rays. He called these unknown rays as X-rays.

Roentgen started different objects between the tube and the fluorescent plate and was able to study several characteristics of X-rays. He was able to publish and reproduce his work and was awarded in 1901 the first Nobel Prize in physics (Hendee et al., 1992). Roentgen recognized the value of his discovery to medicine and was able to produce and publish the first medical. X-ray image, the image of his wife's hand (figure 2.2) in 1896. This discovery of X-ray and its application in medicine paved the way for a new field of medicine called now radiology or diagnostic radiology (Curry et al., 1984).

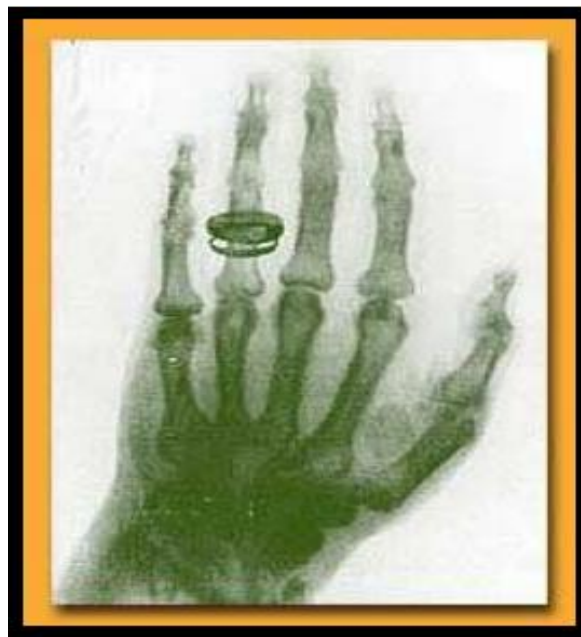


Figure 2.2: Roentgen's wife hand. (rudaw.net 2015)

X-rays now play an important role in health life of all communities. Its examinations are now the most common examination in all hospitals. X-rays are very high frequency electromagnetic radiation or photons. They can be counted individually using Geiger counter which make them seem like particles, But at the same time they diffract like waves when directed at a crystal. This means that X-rays can be treated as particles (photons) or as

waves energy of the wave is dependent on its wavelength λ and the energy of the particle is dependent on its momentum p (Bushong 1993). Thus the energy of a photon (As a wave) (See figure 2.3) may be described either by the equation:

$$E = h \nu = h c / \lambda \quad 2.1 \text{ (Curry, et al., 1984)}$$

Where E is the energy, h is plank's constant, ν is the frequency, c is the speed of light and λ is the wavelength.

Or (as a particle) (see figure 2.4) by the equation:

$$E = P C \quad 2.2 \text{ (Curry, et al., 1984)}$$

Where m is the mAs of the particle and p is its momentum.

$$P = h / \lambda \quad 2.3 \text{ (Curry, et al., 1984)}$$

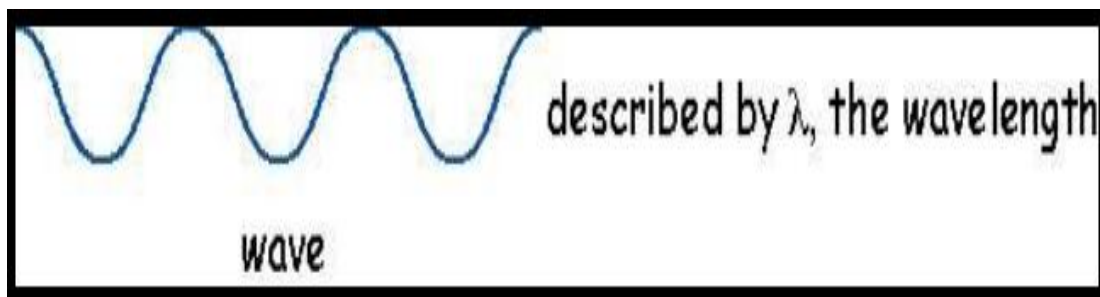


Fig 2.3 the photon as the wave (Curry, et al., 1984)



Figure 2.4 the photon as the particle (Curry, et al., 1984)

X-rays have many properties in common with light. However, the unique properties of X-rays are what make them invaluable in diagnostic imaging. The X-rays are able to penetrate material that absorb or reflect light. When X-rays are absorbed by a certain material, they may produce light. Like light, X-rays can produce an image on a photosensitive film. X-rays can ionize the atoms they pass through and so they can damage cells of the human body when they interact with it. (Bushong 1993)

2.1 Theory of X-ray production:

Any X-ray tube consists of an evacuated glass tube that contains two main components, the cathode and the anode (target). X-ray photons are produced when an accelerated electron hits and interacts with an anode or target material. In the X-ray tube, the cathode (negative electrode) and the anode (positive electrode) are held at very high potential difference. The electrons as a result are accelerated from the cathode to the anode and gain a very high kinetic energy. The electrons are allowed to hit the anode with a very high energy and X-ray photons may be produced (Bushong 1993). The electrons travel with a kinetic energy given by:

$$K = \frac{1}{2}mv^2 \quad 2.4 \text{ (Bushong 1993)}$$

Where m is the rest mass of the electron and v is its velocity

When the projectile electrons travel from the cathode and hit the atoms of the heavy metal anode, they interact with these atoms and transfer their kinetic energy to the target atoms. The projectile electrons interact with either the orbital electrons or the electric field of the nuclei of the target atoms. The interactions result in the conversion of the kinetic energy of the electron into thermal energy (heat) and electromagnetic energy (X-rays) (Bushong 1993).

The accelerated electron interact with the anode via any of the following three processes; excitation, ionization or bremsstrahlung. Each of these processes is discussed separately in the following section.

2.1.1 Excitation:

In this interaction (figure 2.5), the projectile electrons interact with the outer shell electrons of the target atoms, the outer shell electrons get excited and raised to higher energy levels. The outer shell electrons then immediately drop back to the normal energy state with the emission of infrared radiation. In the X-ray tube this emitted infrared radiation heat the anode of the X-ray tube (Bushong 1993).

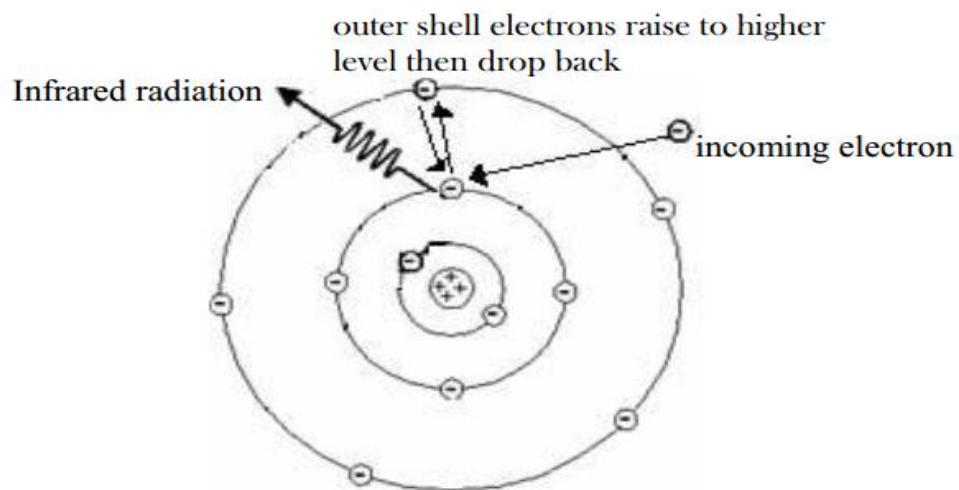


Figure 2.5 Excitation process (Bushong 1993).

2.1.2 Ionization:

In this interaction (figure 2.6), the projectile electrons interact with inner shell electrons where the energy of the incident electrons exceed the binding energy of the electrons in their shells, these inner shell electrons as a result gets ejected from their inner orbits of the target atom and the atom gets

ionized and a hole is created in the place of the ejected electron. This hole is then filled by an electron from a higher energy level and characteristic X-ray lines are produced. These X-rays are called characteristic because its energy is specific to the target. (Bushong 1993)

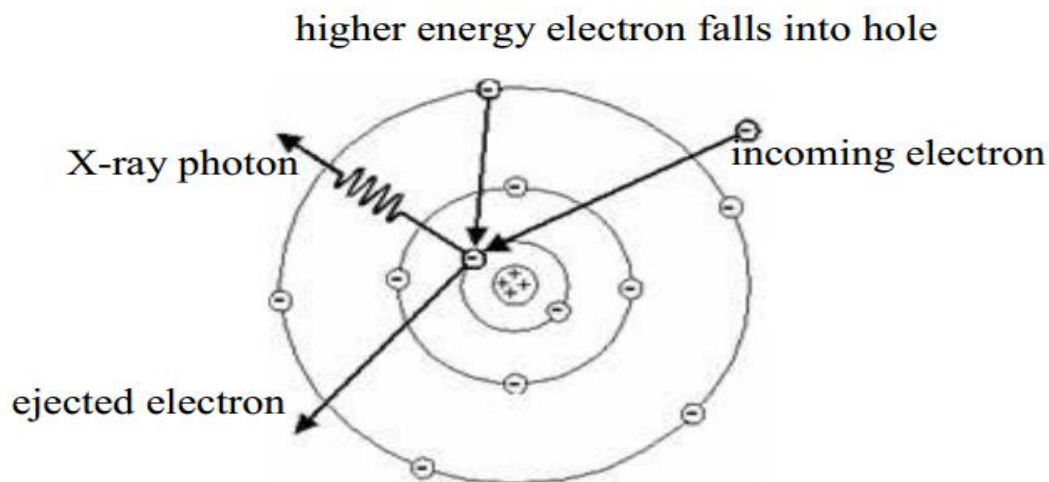


Figure 2.6 Ionization process (Bushong 1993)

2.1.3 Bremsstrahlung:

In this interaction (figure 2.7), the electrons completely avoid the orbital electrons and come sufficiently close to the nucleus of the atom. The electrons are attracted by the strong electric field of the nucleus which causes a sudden change in the motion of the electrons and constitutes a violent deceleration that disturbs the electromagnetic field and a photon is emitted. At each interaction an X-ray is produced, which may have an energy between zero and a maximum value equal to the initial kinetic energy of the incident electron (Bushong 1993).

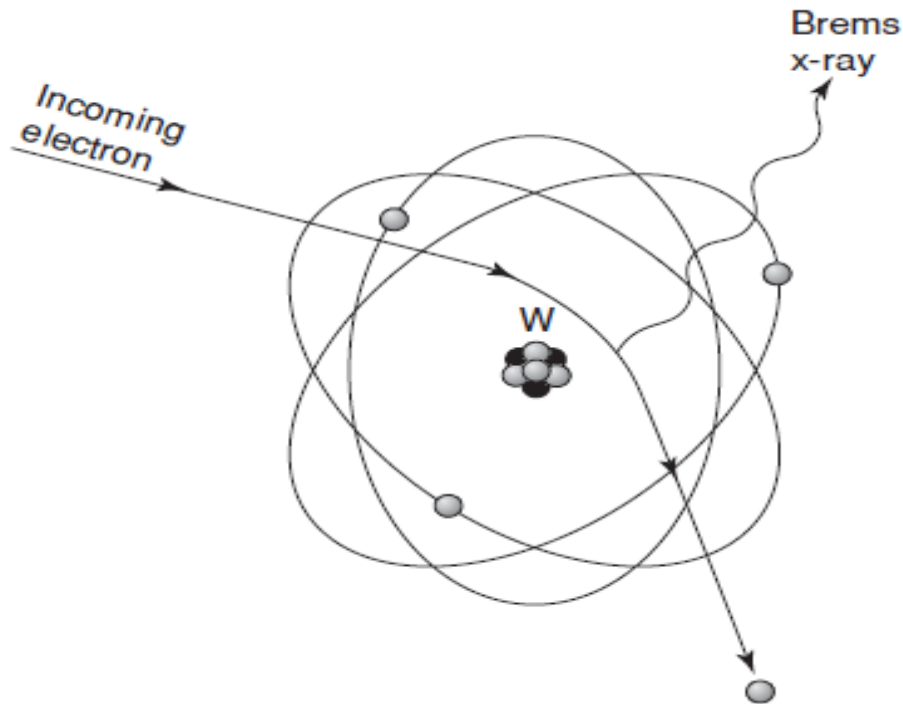


Figure 2.7 Bremsstrahlung process (Saia 2009).

2.2 X-ray spectrum and beam characteristics:

2.2.1 X-ray spectrum:

Figure 2.8 shows a typical X-ray spectrum. This spectrum consists of a continuous spectrum overlapped by number of discrete lines. The continuous spectrum represents Bremsstrahlung X-rays which have energies ranging from zero to a maximum value corresponding to the applied tube voltage. The discrete lines represent the characteristic X-rays which have precise fixed energies and that are produced by target ionization. These energies are characteristic of the differences between binding energies of the particular used element (Bushong 1993).

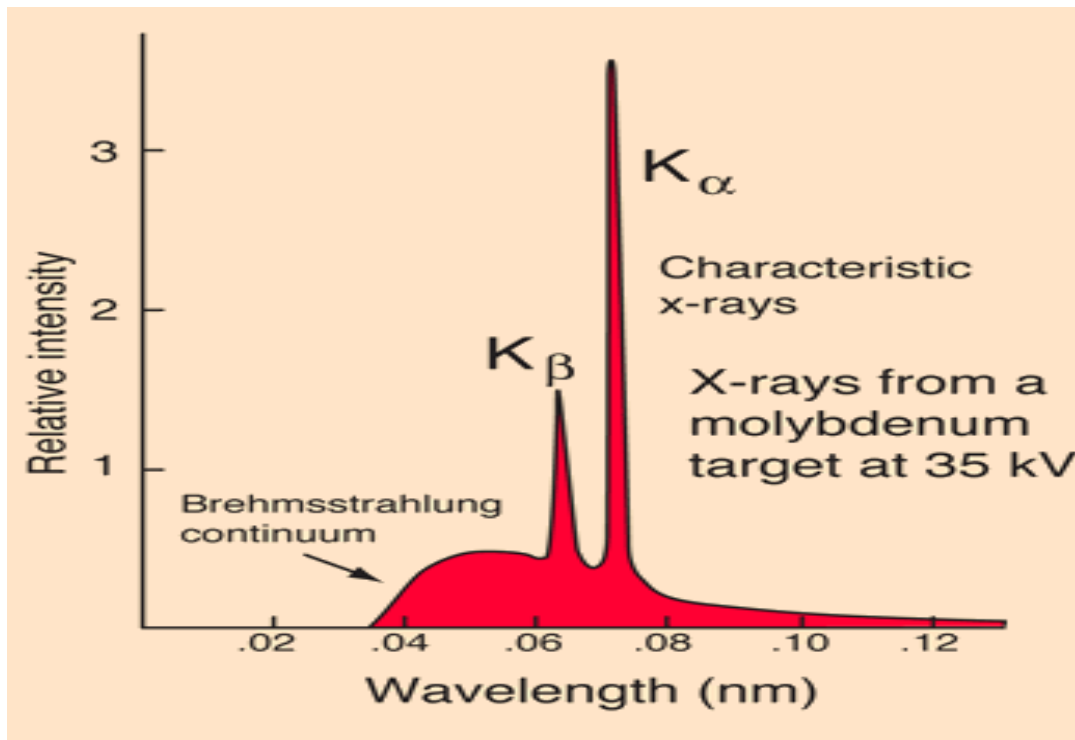


Figure 2.8: Example of X-ray spectrum (Bushong 1993)

2.2.2 X -ray beam characteristics:

X-ray beam can be described by its quality and or its quantity. Each of these characteristics is discussed separately in the following sections.

2.2.2.1 X -ray beam quantity:

The X-ray beam quantity is the X-ray intensity (number of photons per unit area per unit time) or the radiation exposure; and is affected by the change in any of the following factors: Milliampere seconds, kVps and distance and filtration.

Milliamper seconds: (mAs) is the product of X-ray tube current by the time of exposure, it controls the number of electrons accelerated towards the anode. If the current is doubled, twice as many electrons will flow from the

cathode to the target, and hence twice as much X-ray photons will be produced.

Thus, X-ray quantity is directly proportional to the mAs Thus:

$$\frac{I_1}{I_2} = \frac{mAs_1}{mAs_2} \quad 2.5 \text{ (Bushong 1993)}$$

Where I_1 is the X-ray intensity that is produced when a current mAs_1 , is applied on the tube, and I_2 is the X-ray intensity that is produced when current mAs_2 is applied on the X-ray tube. Thus increasing X-ray tube current will also increase X-ray quantity with the same ratio (see figure 2.9)

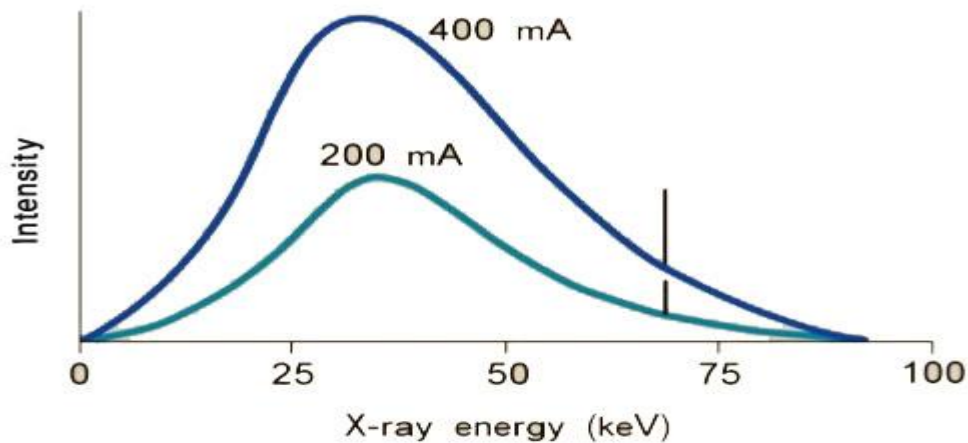


Figure 2.9: Effect of Tube current on X-ray spectrum (Hanan 2007)

Applied voltage (kVp): The increase in the applied voltage will increase the probability of bremsstrahlung interaction and hence more X-ray

Photons will be produced. It was found that X-ray quantity is approximately proportional to the square ratio of the applied voltage (Bushong 1993), thus:

$$\frac{I_1}{I_2} = \left(\frac{kVp_1}{kVp_2} \right)^2 \quad 2.6$$

Where I_1 is the intensity of the beam produced when kVp_1 voltage is applied on the tube and I_2 is the intensity of the beam when kVp_2 voltage is applied on the tube. Any change in the potential will affect both the amplitude and the position of the X-ray spectrum. The area under the curve increases with the square of the factor by which kVp is increased and the relative distribution of emitted X-ray photons shifts to the right (higher energies) (Bushong 1993). Thus for the same mAs increasing the applied voltage will increase X-ray beam quantity.

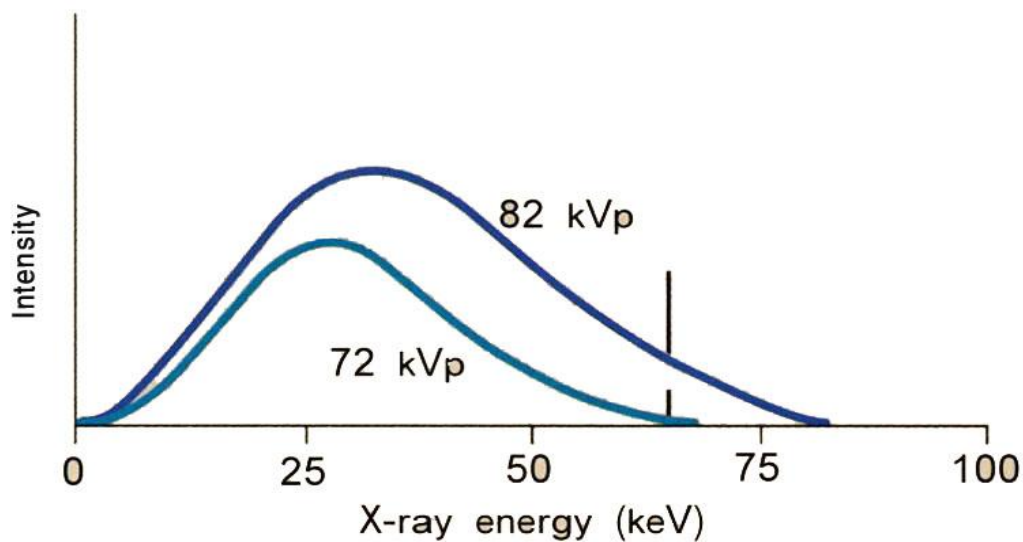


Figure 2.10: Effect of Tube potential on X-ray spectrum (Hanan 2007)

Distance: The intensity of X-rays is inversely proportional to the square distance from the target (Bushong 1993), thus:

$$\frac{I_1}{I_2} = \left(\frac{d_2}{d_1} \right)^2 \quad 2.7$$

Where I_1 is the intensity of the beam when a distance d_1 is used and I_2 is the intensity of the beam when a distance d_2 is used.

Filtration: Any material that lies in the path of the X-ray beam is called filtration. There are two types of filtration; inherent and added filtration. The X-ray tube housing for example is an inherent filter material. Any added material to the beam is called added filtration. Filtration reduces the X-ray quantity by selectively removing low energy X-ray photons that do not add any information to the diagnosing image and hence improving the X-ray beam quality (Bushong 1993). Thus the total effect of filtration on the X-ray beams:

- Change in the X-ray spectrum shape (figure 2.11)
- The peak of the spectrum shifts towards higher energies
- The maximum energy remains unchanged
- The minimum energy shifts towards higher energies

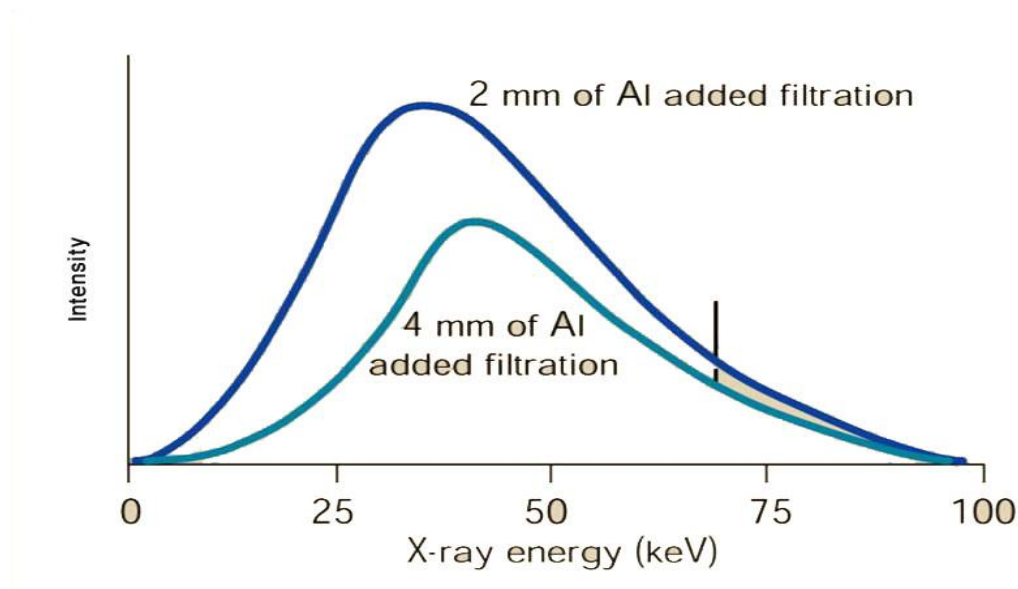


Figure 2.11 Effect of filtration on X-ray spectrum (Hanan 2007)

2.3 X-ray beam quality:

The X-ray quality is a measure of the penetrating ability of the X-ray beam and it is measured by the half value layer (HVL) of the beam. HVL is the thickness of a substance needed to reduce the intensity of the beam into half of its original value. The larger the HVL, the higher the beam quality. The following factors affect the X-ray beam quality:

Applied voltage (Kvp) The kVp controls the speed of the accelerated electrons and therefore controls the energy of the produced X-rays and the half value layer (Bushong 1993).

Target material: The atomic number of the target material affects both the number and the effective energy of the X-rays. When the atomic number of the target is increased, the spectrum is shifted to the right (figure 2.12) (Bushong 1993).

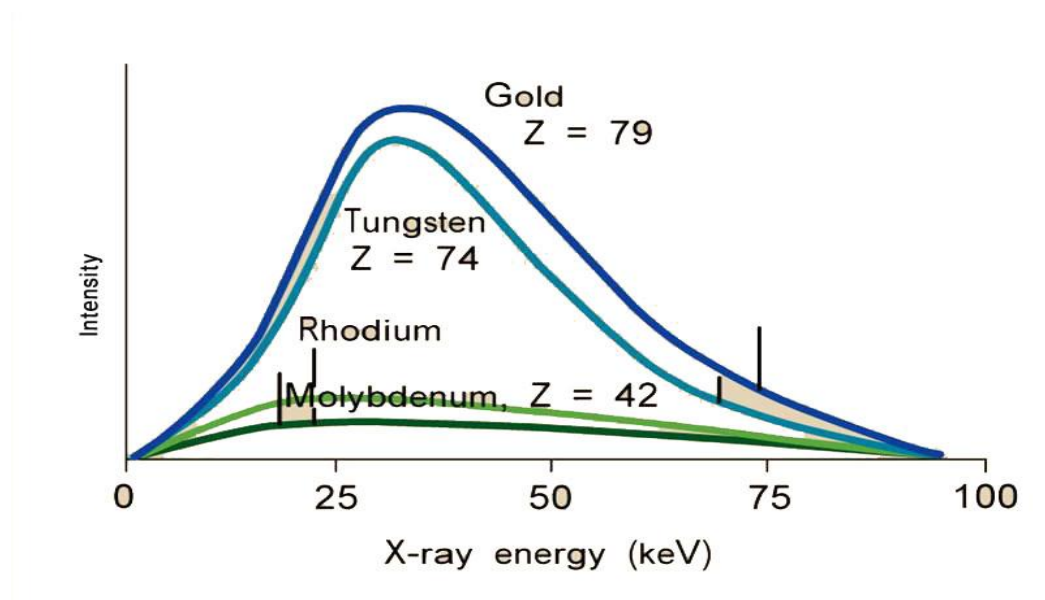


Figure 2.12: Effect of atomic number of target material on X-ray (Hanan 2007) spectrum (Tungsten atomic number = 74, Molybdenum atomic number = 42)

Filtration: the increase of total filtration will increase the beam quality by removing low energy photons.

2.4 Interaction of radiation with matter:

The intensity of an x-ray beam is reduced by interaction with the matter it encounters. This attenuation results from interactions of individual photons in the beam with atoms in the absorber (patient). The x-ray photons are either absorbed or scattered out of the beam. In scattering, photons are ejected out of the primary beam as a result of interactions with the orbital electrons of absorber atoms. Four mechanisms exist where these interactions take place: Coherent scattering, Compton scattering and photoelectric absorption and pair production. In addition, about 9% of the primary photons pass through the patient without interaction to produce the image. (Curry et al.,1984)

2.4.1 Coherent Scattering

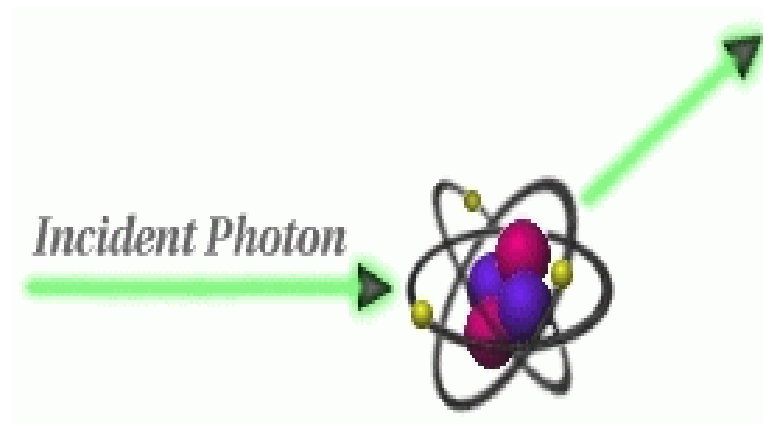


Figure 2.13: Effect Schematic diagram of classical scattering (Curry et al.,1984)

Coherent Scattering (also known as classical scattering and Thompson Scattering) may occur when a low-energy incident photon passes near an outer electron of an atom (which has a low binding energy). The incident

photon interacts with the electron in the outer-shell by causing it to vibrate momentarily at the same frequency as the incoming photon. The incident photon then ceases to exist. The vibration causes the electron to radiate energy in the form of another x-ray photon with the same frequency and energy as in the incident photon effect. Coherent scattering contributes very little to film fog because the total quantity of scattered photons is small and its energy level is too low for much of it to reach the film. (Curry et al.,1984)

2.4.2 Compton scattering:

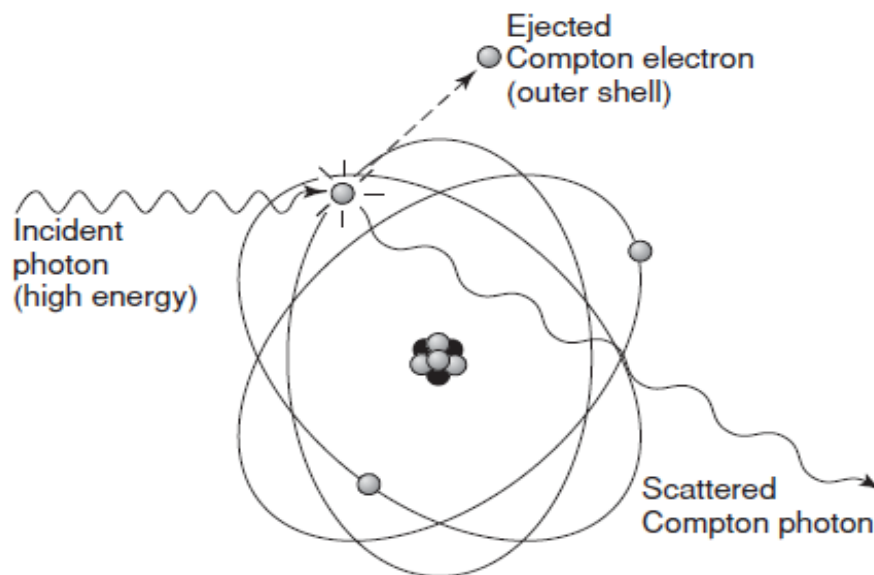


Figure 2.14: Schematic diagram of Compton scattering (Saia 2009)

Occurs when a photon interacts with an outer orbital electron, which receives kinetic energy and recoils from the point of impact. The incident photon is then deflected by its interaction and is scattered from the site of the collision. The energy of the scattered photon equals the energy of the incident photon minus the kinetic energy gained by the recoil electron plus its bonding energy. As with photoelectric absorption, Compton scattering results in the loss of an electron and ionization of the absorbing atom. Scattered photons travel in all directions. The higher the energy of the incident photon, however,

the greater the probability that the angle of scatter of the secondary photon will be small and its direction will be forward. This is advantageous to the patient because some of the energy of the incident x -ray beam escapes the tissue, but it is disadvantageous because it causes nonspecific film darkening (or fogging of the film). Scattered photons darken the film while carrying no useful information to it because their path is altered. (Curry et al., 1984)

The probability of Compton scattering is directly proportional to the electron density. The number of electrons in bone is greater than in water, therefore the probability of Compton scattering is correspondingly greater in bone than in tissue. In a dental x -ray beam, approximately 62% of the photons undergo Compton scattering. (Curry et al., 1984).

The importance of photoelectric absorption and Compton scattering in diagnostic radiography relates to differences in the way photons are absorbed by various anatomic structures. The number of photoelectric and Compton interactions is greater in hard tissues than in soft tissues. As a consequence, more photons in the beam exit the patient after passing through soft tissue than through hard tissue. This allows a radiograph to provide a clear image of enamel, dentine and bone and also, soft tissue. (Curry et al., 1984)

2.4.3 Photoelectric absorption

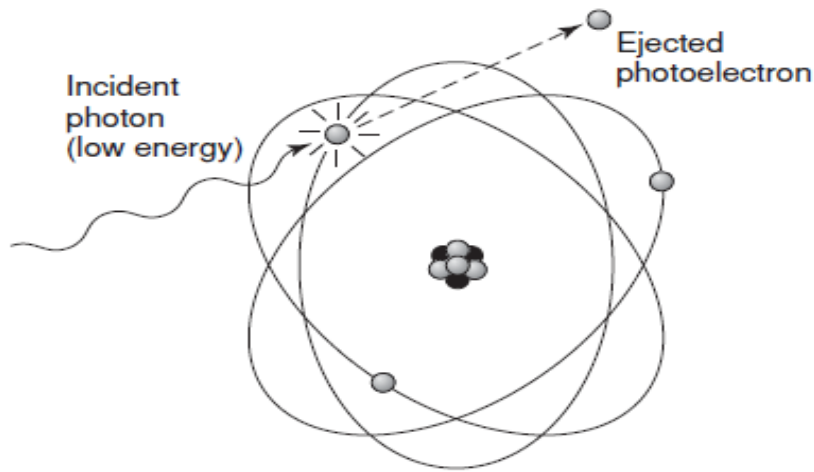


Figure 2.15: Schematic diagram of photoelectric effect (Saia 2009)

Photoelectric absorption occurs when an incident photon collides with an inner-shell electron in an atom of the absorbing medium resulting in total absorption and the incident photon ceases to exist. The electron is ejected from its shell, resulting in ionization and becomes a recoil electron (photoelectron). The kinetic energy imparted to the recoil electron is equal to the energy of the incident photon minus that used to overcome the binding energy of the electron. In the case of atoms with low atomic numbers (e.g. those in most biologic energy of the incident photon. Most Photoelectric interactions occur in the K shell because the density of the electron cloud is greater in this region and a higher probability of interaction exists. (Curry et al.,1984)

An atom that has participated in photoelectric interaction is ionized. This electron deficiency (usually in the K shell) is instantly filled, usually by an L-or M -shell electron, with the release of characteristic radiation. Whatever the orbit of the replacement electron, the characteristic photons

generated is of such low -energy that they are absorbed within the patient and do not fog the film. (Curry et al., 1984)

The recoil electrons ejected during photoelectric absorptions travel only a short distance in the absorber before they give up their energy. As a consequence, all the energy of incident photons that undergo photoelectric interaction is deposited in the patient. This is beneficial in producing high-quality radiographs, because no scattered radiation fogs the film, but potentially deleterious for patients because of increased radiation absorption. (Curry et al., 1984)

The frequency of photoelectric interaction varies directly with the third power of the atomic number of the absorber. For example, because the effective atomic number of compact bone ($Z = 7.4$), the probability that a photon will be absorbed by a photoelectric interaction in bone is approximately 6.5 times greater than in an equal distance of water. This difference is readily seen on dental radiographs. It is this difference in the absorption that makes that production of a radiographic image possible. (Curry et al., 1984)

2.4.5 Pair production:

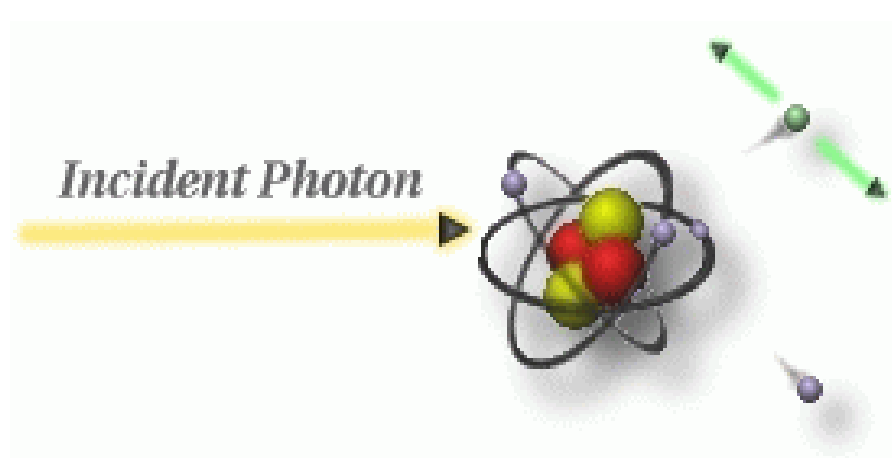


Figure 2.16: Schematic diagram of pair production (Curry et al., 1984)

In this interaction (figure 2.14) a photon with a high energy interacts with the nucleus where the photon disappears and in its place an electron positron pair appears. For this interaction to take place, the energy of the incident photon must be at least 1.02 MeV. This is because the total rest mass of the electron positron pair is about 1.02 MeV/c² (Curry et al., 1984). Because its high energy, this interaction is not important in diagnostic radiology.

2.4.6 Photodisintegration:

In this interaction (figure 2.17) the incident photon has an energy greater than 10 MeV and hence it interacts directly with the nucleus and splits it in parts with emission of neutrons. Because of the high photon energy required for this interaction this interaction does not occur in diagnostic X-ray and as such plays no role (Curry et al., 1984)

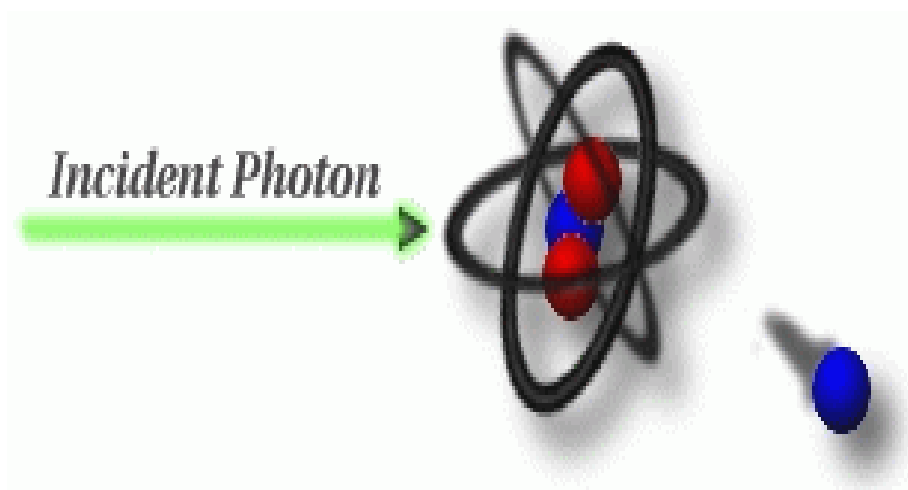


Figure 2.17: Schematic diagram of photodisintegration (Curry et al., 1984)

2.5 Digital radiography (DR):

DR systems encompass a number of different technologies that are rapidly evolving. At this time, the majority of DR systems use thin-film transistor (TFT) arrays, commonly known as flat-panel arrays. Systems based on CCDs are available for general-purpose and chest radiography, using scanned, slot-shaped detectors; a single CCD; or tiled arrays of CCDs optically coupled to larger area x-ray-to-light converters. Thin-film transistor arrays are composed of a matrix of discrete dels, each of which contains a transistor. The transistors operate as gates, permitting an electric charge to flow through them only when they are turned on. During an x-ray exposure, the gates are turned off, and the image is built up in the dels in the form of an electric charge, with the amount of charge in each del proportional to the number of x-rays absorbed in that region of the detector (again, a linear relationship). The means by which x-ray energy is converted to a stored electrical charge varies somewhat between manufacturers but can be broadly classified according to whether it involves an intermediate conversion of x-ray energy to visible photons (indirect flat-panel devices) or not (direct flat-panel devices). In an indirect device, an x-ray-to-light converter, similar to that used in SF imaging, is placed in contact with the TFT array. Each del of the TFT array contains a light sensor (a photodiode) to convert the fluorescent light to a stored electric charge. In a direct device, a layer of material is

deposited directly onto the TFT array. When an x-ray photon is absorbed in this photoconductor material, an electric charge is generated and collected in the del's of the TFT array. For both indirect and direct flat panel detectors, after the x-ray exposure, the TFT array gates are turned on one row at a time, and the amount of charge stored in each del of that row is transferred through drain lines to a row of charge amplifiers at the edge of the array for digitization and storage. The entire detector is read out by successively turning on all of the rows in a sequential fashion and storing the digital data in corresponding locations in the output digital image matrix. (Williams et al., 2007)

2.6 Advantages and Limitations of Digital Radiography:

The main limitations of DR is higher initial cost , a lack of familiarity on the part of both radiologists and technologists with electronic image display and with online soft copy reading (compared with alternator-based batch-mode reading), and the lack of consistent feedback to technologists concerning the use of optimal acquisition techniques. The latter problem, along with the much larger dynamic range of digital systems, has led to a gradual increase in patient radiation dose. The advantages DR include the separation of acquisition, display, and archiving, allowing tremendous flexibility using image-processing functions such as those that adjust the level (analogous to the brightness) and window width (analogous to the contrast) of

the image gray-scale presentation. However, display contrast is limited by the inherent image signal-to-noise ratio (SNR), because as the signal contrast is increased, so is the visibility of noise. Other advantages include: anatomy-specific presentation and disease-specific algorithms; in most cases better x-ray detection efficiency and higher detective quantum efficiency (DQE), permitting lower doses to patients; the ability to use a second computer reader to assist the radiologist; a reduction in the number of image retakes due to underexposure or overexposure; and the elimination of labor-intensive handling and distribution of images during the acquisition process. (Williams et al., 2007)

2.7 Factors affecting image quality:

Just as with SF radiography, a number of factors affect the quality of the image in digital radiography. Contrast, detail, and noise are the primary factors associated with image quality, and they play a major role in CR and DR.

2.8 Detection Efficiency:

For SF, CR, and DR, the efficiency with which incident x-rays are absorbed is determined by the absorber thickness, density, and composition. Efficiency can be increased by increasing material density or absorber thickness (usually at the expense of spatial resolution) or through the incorporation of materials having atomic numbers that provide a good match

between the x-ray spectrum exiting the patient and the absorption characteristics of the material. Figure 2-18 shows the absorption efficiency of 3 materials commonly used as x-ray scintillators, plotted against incident x-ray energy (Williams et al., 2007)

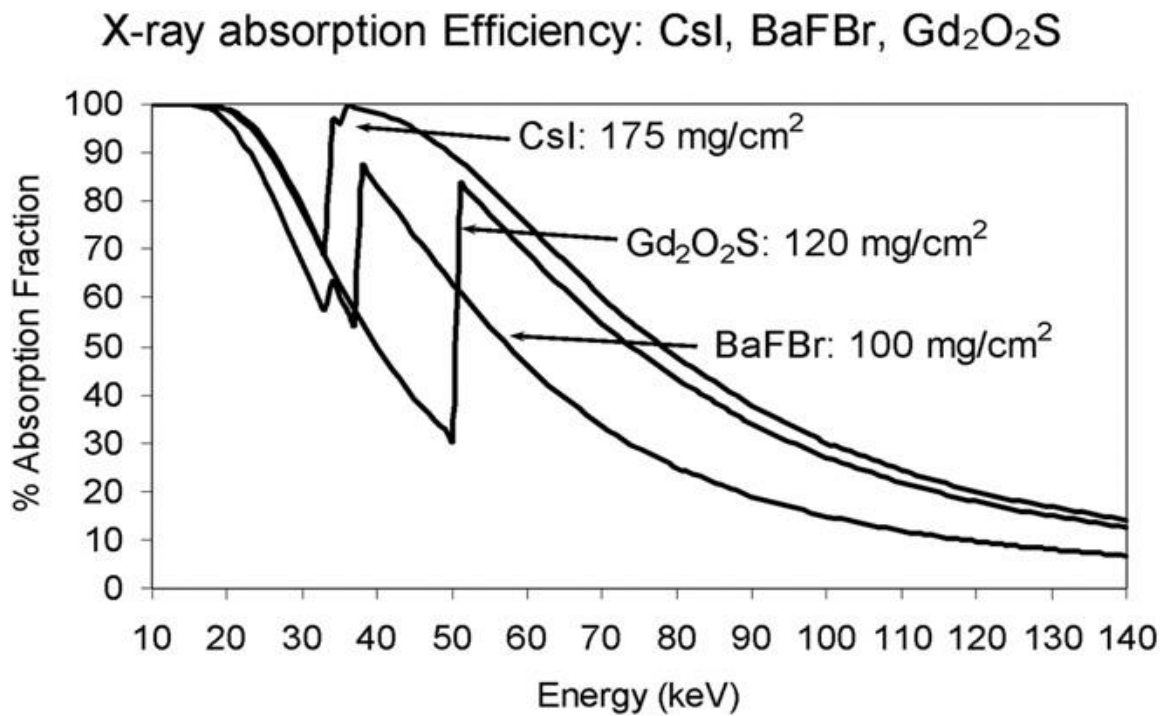


Figure 2-18. The photon absorption fractions (Williams et al., 2007).

Phosphor thicknesses are representative of a standard 400-speed conventional screen, a standard resolution computed radiography phosphor detector (100 mg/cm²), and a cesium iodide phosphor commonly used in indirect thin-film transistor array and optically coupled charge-coupled device camera digital radiography systems (Williams et al., 2007).

2.9 Dose creep in digital radiography and its prevention:

Film-based imaging provides immediate feedback to technologists and radiologists concerning the delivery of the proper radiation exposure to patients. If the optical densities in the film image are too great, the patient received too much radiation, whereas reduced optical densities indicated a reduced radiation exposure relative to the proper value. When digital image receptors replace SF image receptors, the brightness and contrast in the displayed image on the monitor are independent of the exposure used during acquisition. Only the noise in the image changes with the exposure. Radiologists react negatively to digital images with excessive noise (low patient exposure) but rarely complain about images with reduced noise due to excessive patient exposures. Technologists quickly recognize this and gradually increase patient doses by adjusting radiographic techniques upward. This leads to the potential for dose creep in CR and DR. The medical physicist and/or imaging specialist should monitor for dose creep on a consistent, ongoing basis, because it is a recurring phenomenon. One effective way to eliminate dose creep is to develop validated radiographic technique charts for all performed examinations as a function of patient size. If these factors are entered into the anatomic programming of state-of-the-art x-ray generator controls, the technologists simply select the radiologic examination and patient size at the beginning of the case and are assured of the use of

standard radiographic technique factors and standard radiation exposure regardless of whether the examination is conducted with the image receptor on the table top with manual techniques or in the Bucky tray using the automatic exposure control (AEC). (Williams et al., 2007).

2.9 Exposure indicators for digital radiography:

Currently, most CR manufacturers provide exposure indicators on images displayed on the image reader workstation. However, this information may not be transferred over to the picture archiving and communication system (PACS) or may appear buried in the DICOM information page of the patient. Most PACS have the ability to display the exposure indicator on the image. Check with your PACS vendor and insist that this information be displayed on each image. Today, the various numerical exposure indicators used by different CR manufacturers are not easily comparable. To compound the problem further, some DR manufacturers do not provide an exposure indicator on their processed images, or the information is not transferred to the PACS and is not recoverable. (Williams et al., 2007).

The American Association of Physicists in Medicine formed Task Group 116 to address the lack of a uniform exposure indicator on digital radiography images. Their report, “Recommended Exposure Indicator for Digital Radiography,” will propose standardized radiation exposure conditions from which a relative exposure indicator can be defined. Because the major

manufacturers of digital radiographic image receptors participated in the task group, this standardized exposure indicator should migrate into their future products. (Williams et al., 2007)

2.10 Pediatric imaging issues:

As with all pediatric imaging examinations involving ionizing radiation, CR and DR should be performed using the lowest possible radiation exposure to the patient (as low as reasonably achievable (ALARA), because pediatric patients are believed to be up to 10 times more sensitive to ionizing radiation than adults. This suggests that the exposure delivered to the digital image receptor should be approximately 0.4 to 0.8 mR for chest and abdominal examinations (Doyle 1998). However, it should be noted that adopting a policy of reduced exposure levels to the image receptor to achieve ALARA in pediatric imaging increases the possibility of unacceptably high quantum noise and thus reduces the margin for error in the selection of the parameters that affect the beam quality. Also, the achievable reduction in exposure at the plate is dependent on how well the digital system is optimized for pediatric imaging and on the nature of the particular disease being diagnosed (Huda 1996). Commitment and effort on the part of staff members is required to achieve ALARA in pediatric imaging. First, the multiple x-ray machines of a given type in a department require validation, calibration, and matching to ensure the same exposure for similar radiographic technique

parameters. The actual exposure required to produce clinically acceptable images for a given digital receptor is a function of the digital receptor's DQE. The goal is to produce similar image quality in all images regardless of the device chosen and regardless of the size of the pediatric patient. Second, all CR readers or DR image receptors should be adjusted to provide a uniform response to the recorded x-ray image pattern in space. Third, all monitors on all diagnostic display workstations should be tested and calibrated to provide a uniform appearance of displayed images. These topics are addressed in more detail elsewhere (Doyle 1998).

Pediatric patients provide unique challenges when imaged with digital radiography. Uncooperative pediatric patients may require sedation or anesthesia. The range in size from the neonate to the young adult patient requires a wide range in radiographic technique factors and a digital image receptor that properly processes an x-ray pattern in space that may or may not cover the entire image receptor. The decision to use an anti scatter grid must be carefully considered as a function of patient size. Standard positioning aids used to immobilize pediatric patients may generate unacceptable artifacts when used with digital image receptors. Because the x-ray pattern from a pediatric chest compared with an adult chest, for example, has a different dynamic range and other characteristics, display parameters used by the digital acquisition device to properly display the digital image may need to be unique as a function of patient size. Display parameters require further

alteration if gonadal shielding or orthopedic implants appear in the displayed image. Finally, because scoliosis examinations are common in children, the digital image receptor must provide an efficient method to generate images up to 36 inches in length, preferably without doubly exposing some sections of the patient's anatomy.(Poznauskis 2005)

2.11 Proper exposure factors for standard examinations:

Exposure (technique) charts are part of the standard of care expected by the Joint Commission on Accreditation of Healthcare Organizations and are required in many states. For example, in Ohio, exposure charts are required and must include specification of the body part, thickness, and image receptor components to be used for the procedure. Internationally, most countries require regular use of exposure charts. It is necessary to check your county, state, and local regulations for any specific requirements. You may also be required to compute estimates for entrance skin exposures for these charts. Exposure charts are an essential quality assurance component of any diagnostic x-ray imaging department. These exposure guides are especially important in CR and DR, in which the wide exposure latitude makes it possible to obtain clinical images that are severely underexposed, resulting in noisy images, or grossly overexposed, resulting in possible data saturation as well as high patient doses. Improper exposures in digital radiography are more likely to go unnoticed because image processing can correct these

deficiencies to a much greater degree than SF systems because of the wide latitude of the image receptor. Exposure charts are critical in the portable x-ray environment with CR, because manual technique factors are normally required. An underexposed radiograph will have unacceptable noise, while an overexposed radiograph may appear to be of exceptional quality at the expense of patient dose. The first challenge is to understand what constitutes a properly exposed radiograph (Merrill^s 2003). In SF systems, the limited dynamic range of the film determines the exposure latitude. In the digital world, wider exposure latitude can be used to take into account the differing energy responses of the systems and the variability introduced in the dose estimation scheme.. Many CR and DR systems also permit the choice of several exposure (speed) classes. Technique factors for each clinically used exposure class should be constructed. In addition, exposure charts should be designed to function over the wide range of adult patient sizes seen in our clinics today and over the even wider range of sizes found in pediatric radiography. Given a table of body-part thicknesses with suggested technique factors, one can derive, using a spreadsheet program, a full table of values using knowledge of the effect of thickness and kVp on the penetration of the beam. There are also several commercial programs that can be tailored to digital radiography. Typically, the entire exposure chart is calibrated to a single set of exposures based on a common body part, such as the abdomen. A water tank or anthropomorphic phantom can be used to develop appropriate

techniques for the abdominal radiograph. Water works better than acrylic or aluminum because the scatter characteristics are more comparable with the clinical situation. As discussed previously, scatter characteristics can be quite different for digital radiography than for SF. It is also necessary to measure Bucky factors for the under table and wall Bucky assemblies as well as for any snap-on grids (also known as grid caps, portable grids) that may be used with the x-ray machine. Once exposure factors have been determined that result in an appropriate radiograph for the abdomen with the various image receptors, all other values for mAs are interpolated using corrections for distance, Bucky factors, exposure class, patient thickness, and machine output. The exposure chart is then cleaned up by rounding values of mAs to match available mAs stations on the machine. The x-ray output of a portable radiography unit is generally substantially lower than that of a 3-phase or high-frequency stationary x-ray machine. This reduced output capability results in increased exposure times compared with conventional radiography. As a result, patient motion is a common image degradation factor. This factor, coupled with the difficulty in positioning grids correctly in a portable setting, results in frequent exposures being taken without the use of a grid, also degrading overall image quality. (Williams et al., 2007)

2.12 Automatic exposure control:

In CR, photo timers are frequently used with wall and under table Bucky in emergency, inpatient, and outpatient radiology department settings. These AEC units are designed to turn off the x-ray generator when an appropriate exposure level has been received at the image receptor. Automatic exposure controls work well if properly calibrated and properly positioned over clinically important areas of the patient. They fail if placed incorrectly or if pathology in the AEC region of interest causes a significantly different density to be present than expected. Automatic exposure control devices are energy dependent and may require calibration at multiple kVps to function properly over a wide range of patient sizes. Some x-ray generators have preprogrammed energy response curves, and these units may not work as well with CR as with conventional SF receptors because they were probably manufactured to be matched to typical SF energy and scatter characteristics. In this situation, calibrate the wall Bucky for chest work and the under table Bucky for abdominal procedures, or whatever is the most common procedure performed on that image receptor at your institution. In DR, the AEC is normally built into the image receptor assembly, and it works in a manner similar to the photo timers used in SF radiography. However, the number or area of the photosensitive elements may differ from the configurations normally used with conventional SF systems depending on vendor

implementation. Most x-ray generator photo timers are designed to be calibrated for multiple image receptor speeds, usually designated by names such as regular, chest, and detail cassettes. AECs can be calibrated to multiple exposure classes such as 400, 200, and 100 to cover a variety of different CR and DR receptors or specific clinical situations such as pediatrics (Goodsitt 2000). Some CR vendors permit a variety of exposure classes in their software, so the exposure class on the x-ray console must be manually selected to match the exposure class appropriate for that procedure. This can lead to errors if technologists are not vigilant in matching the x-ray generator exposure class to the CR reader exposure class. With some implementations of CR, the AEC unit must be calibrated on the basis of cassette size instead of exposure class. Check with the vendor so that you know which method is most appropriate for you. In DR, the exposure class may also be user selectable, and vigilance is necessary to ensure that technologists are using the appropriate exposure classes, especially for pediatrics. It is usually set automatically in digital radiography systems with an integral x-ray tube assembly. (Goodsitt 2000).

Most digital radiography (cassette-less) systems use an x-ray absorber material coupled to a flat panel detector or a charged coupled device (CCD) to form the image. Therefore an existing x-ray room needs to be retrofitted with these devices if a new DR room is not installed.(Charter et al.,2009)

DR can be divided into two categories: Indirect capture and direct capture

2.13 Indirect capture:

Devices absorb x-rays and convert them into light. The light is then detected by an area-CCD or thin-film transistor (TFT) array and then converted into an electrical signal that is sent to the computer for processing and viewing.(Charter et al.,2009)

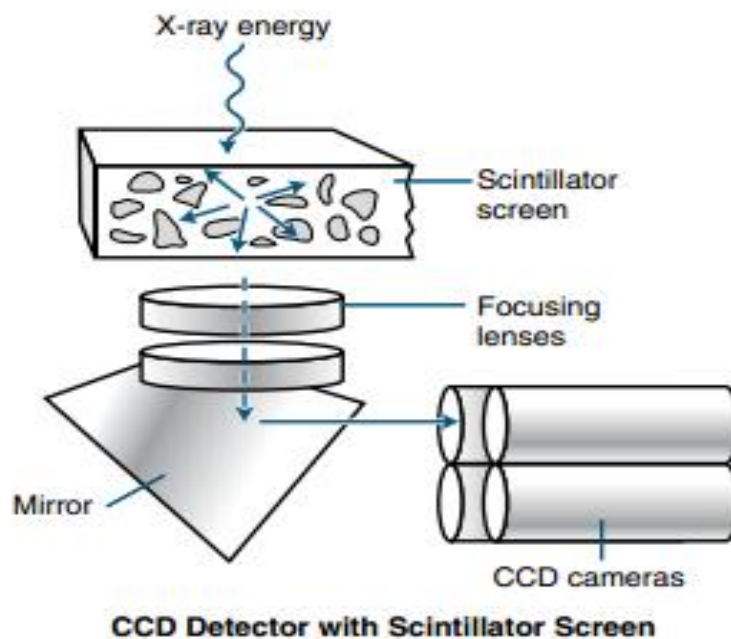


Fig 2.19 the image acquisition process of an indirect capture DR system using CCD technology.(Charter et al.,2009)

2.14 Direct capture:

Devices convert the incident x-ray energy directly into an electrical signal, typically using a photoconductor as the x-ray absorber, and send the electrical signal to the computer for processing and viewing. .(Charter et al.,2009)

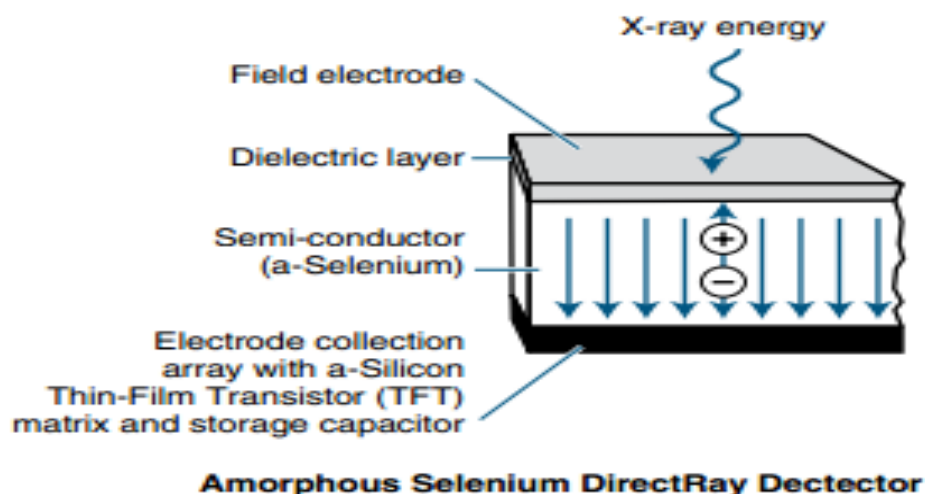


Fig 2.20 The image acquisition process of a direct capture DR system(Charter et al.,2009)

In the early 1970s, several early digital pioneers developed the first clinical application for digital images, digital subtraction angiography (DSA) at the University of Arizona in Tucson. Drs. M. Paul Capp and Sol Nudelman with Hans Roehrig, Dan Fisher, and Meryll Frost developed the precursor to the current full-field DR units. As the technology progressed, several companies began developing large field detectors, first using the CCD technology developed by the military and shortly thereafter using TFT arrays. CCD and TFT technology developed and continues to develop in parallel. Neither technology has proven to be better than the other. (Charter et al., 2009)

2.15 Comparison of CR and DR with Conventional Radiography:

When comparing film/screen imaging with CR and DR, several factors should be considered. For conventional x-ray and CR, a traditional x-ray room with a table and wall Bucky is required. For DR, a detector replaces the Bucky apparatus in both the table and wall stand. Because both conventional radiography and CR use cassettes, technologists often rate them the same in

terms of ease and efficiency, but DR has an advantage because the processing is done right at the room's console. The image will appear in 3 to 5 seconds, and the technologist knows right away if the image needs to be repeated.

Latent image formation is different with conventional radiography, CR, and DR. In conventional radiographic imaging, a film is placed inside a cassette that contains an intensifying screen. When the x-rays strike the intensifying screen, light is produced. The light photons and x-ray photons interact with the silver halide grains in the film emulsion, and an electron is ejected from the halide. The ejected electron is attracted to the sensitivity speck. The speck now has a negative charge, and silver ions are attracted to equal out the charge.(Charter et al.,2009)

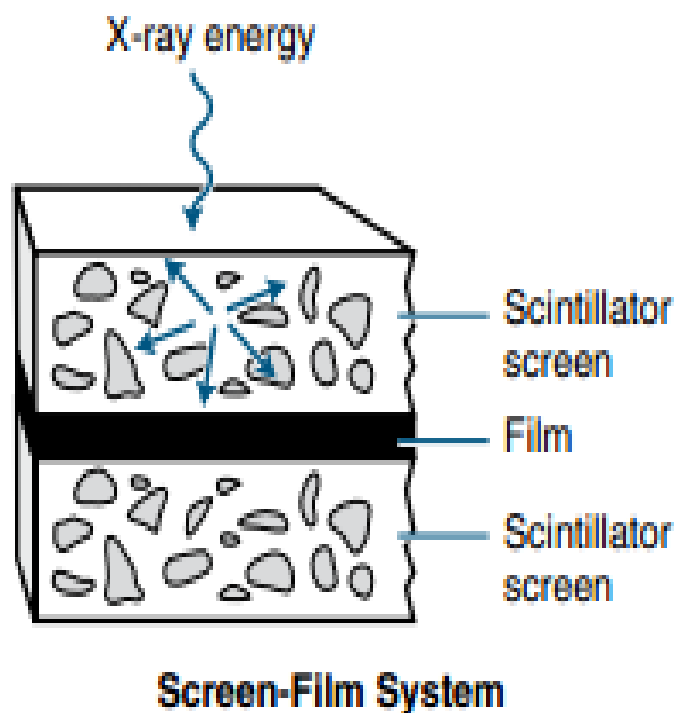


Fig 2.21 Conventional radiography latent image formation (Charter et al., 2009)

This process happens many times within the emulsion to form the latent image. After chemical processing, the sensitivity specks will be processed into black metallic silver, and the manifest image is formed.

In CR, a photostimulable phosphor plate is placed inside the CR cassette. Most storage phosphor plates today are made of a barium fluorohalide (where the halide is bromine and/or iodine) with europium as an activator. When x-rays strike the photostimulable phosphor, some light is given off, as in a conventional intensifying screen, but some of the photon energy is deposited within the phosphor particles to create the latent image

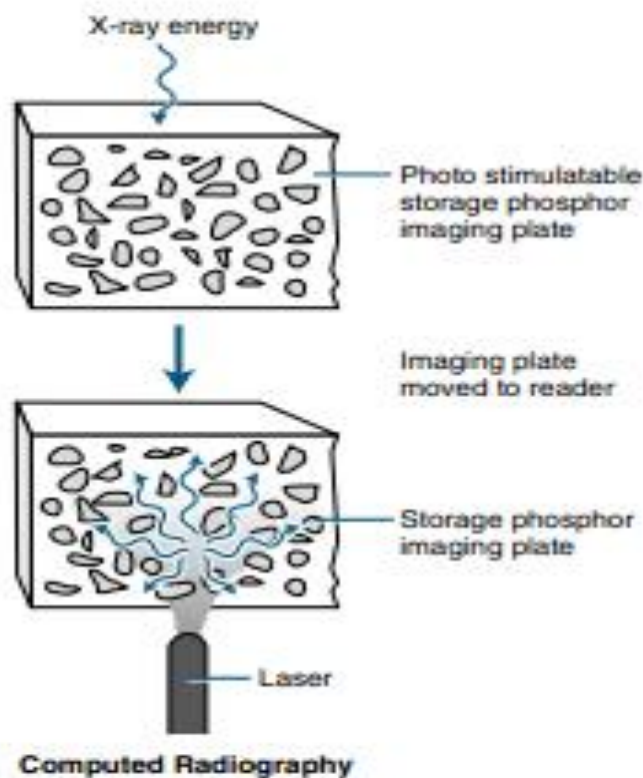


Fig 2.21 CR latent image formation (Charter et al., 2009)

The phosphor plate is then fed through the CR reader. To release the latent image, focused laser light (from one or more lasers) is scanned over the plate, causing the electrons to return to their original state and emitting light in the process. This light is picked up by a photomultiplier tube and converted

into an electrical signal. The electrical signal is then sent through an analog-to-digital converter to produce a digital image that can be sent to the technologist review station.(Charter et al.,2009)

In DR there are no cassettes. The image acquisition device is either built into the table and/or wall stand or enclosed in a portable device. There are two distinct image acquisition methods: indirect capture and direct capture. Indirect capture is very similar to CR in that the x-ray energy stimulates a scintillator, which gives off light that is detected and turned into an electrical signal. With direct capture, the x-ray energy is detected by a photoconductor that converts it directly to a digital electrical signal.(Charter et al.,2009)

Image processing in conventional radiography is done with chemicals and the shape of the film's response curve. With CR and DR, image processing takes place in a computer. For CR the computer is located near the readers, whether there are several readers distributed throughout the department or there is one centrally located reader. For DR the computer is either located next to the x-ray console or is integrated within the console, and the image is processed before moving on to the next exposure. (Charter et al., 2009)

The exposure latitude or dynamic range used in conventional radiography is based on the characteristic response of the film, which is nonlinear. Acquiring images with CR or DR, on the other hand, involves using a detector that can respond in a linear manner. The exposure latitude is very wide because a single detector can be sensitive to a wide range of exposures. In conventional radiography, radiographic contrast is primarily controlled by kilovoltage peak (kVp). With CR and DR, kVp still influences subject contrast, but radiographic contrast is primarily controlled by an image processing.(Charter et al.,2009)

2.16 Previous studies:

Digital radiography examinations play an important role in the health care of the population worldwide. These examinations may involve significant irradiation of the patient and probably represent the largest man-made source of radiation exposure for the population. Radiation has been long known to be harmful to humans. The radiation exposure received in X-ray examinations is known to increase the risk of malignancy as well as, above a certain dose, the probability of skin damage and cataract.

In today's diagnostic radiology, there is a growing concern about radiation exposure. This can be seen in the recommendations of the International Commission on Radiation Protection (ICRP publication 60, 1991) and many other 30 national publications. All these recommendations advice that X-ray examinations should be conducted using techniques that keep patients doses as low as compatible with the medical purposes of the examinations. In order to achieve this recommendation, it is necessary to understand the factors that affect the exposure and to be able to evaluate patient's doses.

Intensive studies in the field of patient dose were conducted in the world. All these studies eventually lead to the introduction of the European Union Council Directive (EUCD) which made it compulsory that patient's dose be measured in every hospital and those doses should be compared to reference dose levels established by the competent authorities.

The need for standardization of radiation exposure and guidance levels for various radiographic examinations has also been proposed by the International Atomic Energy Agency (IAEA) as a safety standard (IAEA Safety Series No. 115-1, IAEA, Vienna 1994). The guidance levels by IAEA are based on UK and European studies. Several guidelines and dose reference

levels were also published by number of international organizations and was recently summarized by ICRP .These guidelines have stimulated worldwide interest in patients' doses and several major dose surveys have been conducted (Geleijns .,1998 et al).

Patient dose has often been described by the entrance skin dose (ESD) as measured in the centre of the X-ray beam. Because of the simplicity of its measurement, ESD is considered widely as the index to be assessed and monitored. ESD is measured directly using Thermo luminescence Dosimeter (TLD) placed on the skin of the patient or indirectly from the measurements of dose-area product using a large area Transmission Ionization Chamber (TIC) placed between the patient and the X-ray tube. (McCullough et al., 1970).

The use of TLD method in ESD assessment is a time consuming process.TLD technique requires prolonged annealing and reading process, Furthermore, the use of TLD technique requires special equipments and thorough calibration facilities which may not be available in most X-ray departments. On the other hand TIC method does not provide direct measurement of skin dose and mathematical equations are needed to convert TIC reading into Skin dose.

Because of the limitations associated with both TLD and TIC, several mathematical equations have been suggested to relate skin dose to the used exposure factors such as the applied mAs, surface to skin distance (SSD), filtration, field size, output, and the applied kVp . These equations provide an easy and more practical mean of estimating skin dose even before exposure. They also provide the easiest and cheapest technique can be employed in any kind of patient dose survey or audit. Despite the attractive nature of the calculation methods of patient dose, one should make sure that the used X-ray

equipment has an adequate QC protocol that ensures the accuracy of the measured exposure factors.

The Assessment of Entrance Skin Dose in routine x-ray examinations of chest, skull, abdomen and pelvis of children in five selected hospitals in Nigeria this study assumed that children are more susceptible to the effects of ionizing radiation and so deserves special attention. Entrance skin doses (ESD) and Effective dose (E) to pediatric patients were estimated during chest, skull, abdomen and pelvis examination in five Nigeria hospitals using DoseCal software. The mean ESD for Chest (PA) in age range 1 – 5 in the five hospitals (H1 – H5) were 70, 139, 130, 105 and 111 μ Gy, respectively. The median ESD values in all the examinations were compared with the NRPB and EC reference level and were found to be lower except for Chest PA and Chest Lateral examinations. The mean effective doses were compared with those found in literature and were found to be comparable. (Ademola et al., 2013).

In many hospitals a routine chest X-ray (CXR) is frequently performed exam specially for evaluating Pneumonia. The objectives of study were to evaluate Entrance skin dose (ESD) in pediatric CXR posterior-anterior (PA) and lateral (Lat) projection and also to estimate organs radiation doses. 100 patients underwent chest x-ray, in Taif pediatric hospital in Taif, KSA, their age range from 0-15 years. The patients biodata (age, weight, height, Gender and body mass index (BMI)) were recorded. The exposure factors, focal skin distance, tube output and back scatter factor were entered in special software known by DOS CAL in order to calculate the ESD. The range of Kilovoltages and ESDs obtained were 40- 63kVp and 0.11-0.56 mGy respectively per radiograph for different ages and groups and both intended chest views. Significant correlation coefficients were found between tube potential, patients weight and ESDs. The mean radiation dose in lateral chest was 0.31 ± 0.05

mGy. Skin and lung absorbed more radiation dose than other organs. The results of radiation dose for pediatric chest in this study matched and compatible with literature. The results presented will serve as a baseline data needed for deriving local reference doses for pediatric chest X-ray examinations. (Osman 2013).

A survey of the entrance surface doses in the routine radiography of children in eastern Nigeria has been carried out in three hospitals, using thermoluminescence detectors. Chest, abdomen, lumbar spine, skull and pelvis were covered in this study. Findings reveal that doses are higher than the recommended reference values elsewhere, as well as values reported for Sudan. The mean percentage difference in entrance doses for chest radiography for this study and an earlier one carried out for three hospitals in the west of Nigeria is about 44.7%. The high doses are traceable to a lack of standardization in procedures, resulting in use of low tube voltages and high currents for examination, as well as the status of facilities in the area. Recommendations are made for immediate corrective measures to lower the doses. (Egbe 2008)

2.17 Calculation methods of entrance skin dose:

The first set of skin dose calculation was published by Birtch et al in 1974 (Birtch et al., 1979). A more simple equation of skin dose was then published by Edmond (IR Edmonds 1984) in 1984. Edmonds used the data published by Birtch and proved that these radiation doses can be reduced to a simple function that depends on kVp, mAs, filtration and SSD. Edmonds noted that skin dose is proportional to $(kVp)^{1.74}$ and as such, skin dose may be given by: (Birtch et al., 1979)

$$skin - dose(\mu Gy) = \frac{836(kVp)^{1.74}(mAs)}{(SSD)^2} \left(\frac{1}{T} + 0.114 \right) \quad 2.8$$

Where T is the total filtration in mm Aluminum, SSD is the source to skin distance in cm, and kVp is the applied kilo voltage.

The second studies by Shrimpton (Shrimpton 1985) who compared the results obtained using Edmonds formula with that obtained by direct measurement of skin dose using TLD. Shrimpton noted that Edmond's formula produce an estimate of air kerma in the absence of patients, and its use in estimating skin dose may involve significant error. The second trace of skin dose can be found in the literature was the two formulas published by Tung and Tsai in 1999 (Tung et al., 1999). Similar to the approach used by Edmonds (Edmonds 1984), Tung and Tsai studied the relationship between 34 entrance skin dose and X-ray tube potential and between entrance skin dose and Aluminum filtration. These two relations allowed Tung and Tsai to propose the following equation for three phase X-ray generators:

$$ESD = c \left(\frac{KVp}{FSD} \right)^2 \left(\frac{mAs}{mm.Al} \right) \quad 2.9 \text{ (Edmonds 1984)}$$

Where ESD is the entrance skin dose, kVp is the applied tube potential, mAs is the applied mAs (tube current multiplied by exposure time), FSD is the focus to skin distance, and c is the proportionality constant or machine dependant constant which depends on the X-ray machine and is about 2.775 for all manufacturers and X-ray machines studied by Tong and Tsai.

Also the dose may calculate by the dose calculation system that designed to calculate and report entrance surface dose. By determining the tube output data and exposure factors encountered. Using equation 1 (Suliman 2008)

$$ESD = OP \times \left(\frac{kV}{80} \right)^2 \times mA \times s \times \left(\frac{100}{FSD} \right)^2 \times BSF$$

2.10 (Suliman 2008)

Where (OP) is the output in mGy/ (mA s) of the X-ray tube at 80 kV at a focus distance of 1 m normalized to 10 mA s, (kV) the tube potential, (mA s) the product of the tube current (in mA) and the exposure time (in s), (FSD) the focus-to-skin distance (in cm) and (BSF) the backscatter factor. The normalization at 80 kV and 10 mA s was used as the potentials across the X-ray tube and the tube current are highly stabilized at this point. BSF is calculated automatically by the Dose Cal software after all input data are entered manually in the software. The tube output, the patient anthropometrical data and the radiographic parameters (kVp, mA s, FSD and filtration) are initially inserted in the software. The kinds of examination and projection are selected afterwards. (Tung et al., 1999).

CHAPTER THREE

3. Materials:

3.1 Population of the study:

The study population was composed of pediatrics (2-15 years) presenting to the Aseer central Hospital in Abha- KSA during the period from August 2013 to August 2015.

3.2 Study sample:

The sample size consisted of 152 patients.

3.3 Inclusion criteria

Pediatrics patient (2-15) years

3.4 Exclusions criteria

- Pediatric patients less than 1 year in age.
- Pediatric patients more than 15 years in age

3.5 Ethical consideration:

Special consideration was given to the right of the confidentiality and anonymity for all participants. Anonymity was achieved by using number for each participant to provide link between the collected information and the participants. In addition confidentiality was obtained by making the collected data accessible only to the researcher and the supervisor. Justice and human dignity was considered by teaching the selected participant equally when offering them an opportunity to participate in the research. Permission for

conducting the study was obtained from head of the radiology department in Aseer central hospital.

3.6 Data analysis:

Data were presented as mean \pm SD in a form of comparison tables. Statistical analysis was performed using the standard Statistical Package for the Social Sciences (SPSS Inc., Chicago, IL, USA) version 16 .ANOVA and person correlation, Independent t-test were used. Correlation is significant at the $p < 0.05$

3.7 The machine used:

The equipment requirements included a digital radiography , Manufactured for GE Health care, Milwaukee,wi By Siemens, S.N : 4927, Model : ALOIC II, Manufactured : February / 2013, Location : Kemnath / Germany, Type : 5234954, Filtration : 2.0 mm Al / 70 KV, Localizer Lights : 24 v , 150 W.



Fig 3.1 DR machine from GE Health care, Milwaukee,wi By Siemen,
(manual 2013)

The machine consists of the basic form of the following components:

- Ceiling support with x-ray tube assembly, collimator and control panels
- Ceiling support with detector
- Patient table with new designed table tops (for example for children).
- Standing console with computer, display, keyboard, mouse and manual radiation release (digital imaging station with the FD imaging system).
- Control cabinet with detector electronics and generator cabinet.

3.8 Methods:

3.8.1 X-ray technique used:

Different radiological examinations including : Foot ,AP Pelvis, Skull PA ,PA Hand ,AP Arm ,Ankle, AP Shoulder , Forearm ,AP Femur, AP Elbow, were included ,these examinations were obtained using fine focus and FFD of 100cm.Chest PA and Abdomen were obtained by using broad focus and FFD180 -100cm respectively. Patient information including age ,gender ,weight ,BMI ,height was considered .The type radiological examination and applied projection as well as the exposure details such as tube voltage (KV),tube current (MAS) ,organ thickness, focal to skin distance (FSD)were evaluated.

3.8.2 Measure of the entrance skin dose:

The ESD was calculated according to the following equation which was applied by (Tung and Tasi; 1999).

$$ESD = c \left(\frac{KVp}{FSD} \right)^2 \left(\frac{mAs}{mm.Al} \right) \quad 2.11$$

Where:

ESD stands for Entrance skin dose, $c = \text{constant} = 0.2775$, Kvp=Applied Tube potential, mAs =Tube current multiplied by exposure time, FSD=Focus to skin distance, Al=Aluminum Filtration

3.8.3 Data collection:

The data was collected by master data sheets using the variables of age, gender, weight, BMI, height, type of examination, projection, parameters (tube voltage (kvp), tube current (MA), time of exposures (sec), distance and focus) and select one method of assessment (Equation) to measure the entrance skin dose.

CHAPTER FOUR

4. Results:

Table 4.1: The mean and \pm SD values of all the pediatrics examined in the study

	Age (Year)	Weight (Kg)	BMI	Height (Cm)	Tube Voltage (KV)	mAs (Ma)	organ thickness (Cm)	FSD (Cm)	ESD (mGy)
N	152	152	152	152	152	152	152	152	152
Mean	7.5875	23.086	16.4644	117.546	62.6645	5.5059	6.8592	100.311	.35583
Median	8.0000	24.000	15.9600	123.000	63.0000	5.5000	5.0000	96.0000	.29900
Std. Deviation	4.6492	6.9434	2.69886	15.5046	6.11149	1.77951	3.93447	21.1243	.180796
Minimum	2.00	11.00	12.19	86.00	46.00	2.00	2.00	85.00	.005
Maximum	55.00	51.00	27.34	140.00	76.00	10.00	16.00	170.00	.919

Table 4.2: Mean and standard deviation for ESDs in mGy for the radiological examinations (projections)

Descriptive						P -value
EDDs						
	N	Mean	Std. Deviation	Minimum	Maximum	
AP	78	.40036	.195010	.086	.919	0.000
Dorsi planter	9	.15917	.074292	.005	.245	
lateral	55	.35035	.148750	.017	.621	
oblique	10	.21570	.086778	.023	.301	
Total	152	.35583	.180796	.005	.919	

Table 4.3: Mean and standard deviation for ESDs in mGy for the radiological examinations (part under examination)

Descriptive						P -value
ESDs						
	N	Mean	Std. Deviation	Minimum	Maximum	
Chest	14	.16807	.053513	.113	.329	0.000
Foot	12	.20608	.068993	.017	.289	
Pelvis	6	.62017	.186844	.409	.919	
Skull	21	.58681	.087694	.422	.770	
Hand	24	.20344	.097389	.005	.467	
Arm	13	.26162	.041989	.173	.323	
Ankle	10	.44170	.112397	.231	.576	
Shoulder	6	.46067	.159019	.284	.641	
Abdomen	17	.52776	.092996	.296	.644	
Forearm	7	.21500	.030067	.189	.259	
Femur	11	.35600	.097196	.086	.444	
Elbow	8	.28650	.022558	.277	.342	
Knee	3	.35567	.031786	.320	.381	
Total	152	.35583	.180796	.005	.919	

Table 4.4: Mean and standard deviation for ESDs in mGy for the radiological examinations (Age class)

Descriptive						P -value
ESDs						
	N	Mean	Std. Deviation	Minimum	Maximum	
2-5 y	40	.28080	.148638	.023	.693	0.009
6-9 y	88	.38351	.178684	.005	.770	
≥10 y	24	.37942	.207518	.150	.919	
Total	152	.35583	.180796	.005	.919	

Table 4.5: Mean and standard deviation for ESDs in mGy for the radiological examinations (gender)

Descriptive						P -value
ESDs						
	N	Mean	Std. Deviation	Minimum	Maximum	
Male	78	.35129	.185812	.005	.770	0.752
Female	74	.36062	.176494	.086	.919	
Total	152	.35583	.180796	.005	.919	

Table 4.6: Weight, BMI and Height

Correlations		
		ESD
Weight	Pearson Correlation	.127
	Sig. (2-tailed)	.119
	N	152
BMI	Pearson Correlation	-.152
	Sig. (2-tailed)	.062
	N	152
Height	Pearson Correlation	.251(**)
	Sig. (2-tailed)	.002
	N	152

Correlation is significant at the 0.01 level (2-tailed).

Table 4.7: Tube Voltage (KV), mAs, Organ thickness and Distance (FSD))

Correlations		
		ESD
Tube Voltage (KV)	Pearson Correlation	.485(**)
	Sig. (2-tailed)	.000
	N	152
mAs	Pearson Correlation	.752(**)
	Sig. (2-tailed)	.000
	N	152
Organ thickness	Pearson Correlation	.503(**)
	Sig. (2-tailed)	.000
	N	152
Distance (FSD)	Pearson Correlation	-.450(**)
	Sig. (2-tailed)	.000
	N	152
*. Correlation is significant at the 0.05 level (2-tailed).		
**. Correlation is significant at the 0.01 level (2-tailed).		

CHAPTER FIVE

5. Discussion

The mean and \pm SD values of all the pediatrics examined in the study were presented in (table 4.1). Study population comprised 152 pediatric patients (78 males and 74 females). their ages ranged from 2 to 15 years; with a mean age of (7.58 ± 3.10) years , weight ranged from 21to 51 Kg; with a mean value of (23.0862 ± 7.86) years , mean height of (117.5461 ± 17.36) years , height ranged from 86 to 140 cm; the smallest BMI of the population was 12.19 and the largest value was 27.34.

The mean and \pm SD of the Digital Radiography X-Ray machine parameters were presented in (table 4.1). The maximum Kv was found to be 76, mAs of 10, organ thickness 16 cm, Focus to Skin Distance (FSD) of 170 and the measured ESD was of 0.919.

Mean and standard deviation for ESDs in mGy for the radiological examinations were compared with other authors, and were presented in (table 4.3), The maximum ESD was found in the AP pelvis (0.919 ± 0.26) and the minimum dose was found in PA hand (0.15 ± 0.05) . It was found that the dose level received by the digital radiography machine in our hospital were lower than other studies levels (EC 1996), (NRPB 2000), with significant difference at $p < 0.000$ in respected to different type of X-ray examinations. The justification may be due to the fact that the digital X-ray machine (Siemens) was manufactured with high engineering technology and gave low doses because of the cathode cup is optimized for use in a line-focus, planar anode tube and has a slot in which the emitter is situated. It can be seen in Table 3 that The ESD (mGy) for the PA chest was close to that reported by the (NRPB, 2000) mGy but lower than the value of (EC 1996) by 0.14mGy .The

ESD (mGy) for the AP pelvis was lower than the value that reported by European Committee (EC 1996) by 3.7mGy due to, may be the patients thickness under study. The ESD (mGy) for abdomen half than value recorded by The European Commission (EC 1996) and close to that values reported by National Radiological Protection Board (NRPB, 2000) and IAEA (IAEA, 1996)

Similar examinations carried out in Sudan at four hospitals, eight X-ray units, their hospital mean ESDs estimated range from 0.17 to 0.27 mGy for chest AP, 1.04 - 2.26 mGy for Skull AP/PA.

The radiological technique including AP, Dorsi planter, lateral and oblique projections have no impact on the ESDs measures it ranged between 0.15-0.33mGy Dorsi planters and oblique have less ESD than other projections (table 4.4)

The maximum pediatric age class was found at ages between 6-9 years, they constituting 23 pediatric patients. The maximum ESD received was for pediatric of ages of 10 and more, however there is no significant relation between age classes and ESD (see table 4.5)

Gender and body characteristics including weight, height, BMI, have no impact on the ESDs, however the organ thickness has a significant relation with ESD at $p < 0.000$. Tables (4.6) and (4.7).Correlations between Entrance Skin Dose (ESD) and Exposure parameters showed significant relation, table (4.7).Many authors stated that the absorbed dose in skin is directly proportional to tube current; the length of exposure, and the square of peak kilovoltage. the justification was that the digital imaging X-ray machine may allow for use of a lower tube current or a shorter exposure, thus reducing the dose to the patient as mentioned by (Parry, et al., 1998) and where the Image

quality controlled automatically because the using of automatic exposure control as well as the presence of Aluminum Filter of 2.0mm.

However, the risk from radiation exposure of the patients must be balanced versus the diagnostic benefit. Many departments do not use recommended radiographic parameters for children using digital radiography, Furthermore, wide variations in the applications of the radiographic techniques, equipment performance at different hospitals over the world.

5.1 Conclusion:

This study performed in Saudi Arabia at Asser Central Hospital-KSA ;is considered as an attempt to evaluate the ESDs received by digital radiographic x-ray machine for children aged between 2-15 years old. For all the examinations studied in the hospital, the mean ESD values obtained are found to be within the standard reference values of doses. The data obtained may add to the available information in national records for general use. The guidance on where efforts on dose reduction will need to be directed to fulfill the requirements of the optimization process and serve as a reference for future researches and in pediatrics of ages less than two years old.

5.2 Recommendation:

- - Pediatrics radiology should be governed with high professional's techniques to minimize radiation hazard on children while they are examined by X-ray.
- - Dose to the patient should be at the lowest level that still guarantees a sufficient diagnostic image quality.
- - Check digital radiography machine regularly to insure the output from the machine at exactly level according to QA program.
- - At any radiology department must prepare parameters chart.
- - We must follow the NCRP recommendations that dealing with minimizing patient dose.
- - Further studies are needed to assess and measure ESDs to keep it at reference levels.

REFERENCES

Ademola IOSR Journal of Applied Physics (IOSR-JAP) e-ISSN: 2278-4861. Volume 5, Issue 2 (Nov. - Dec. 2013), PP 47-50.

Annals of the ICRP: Risks associated with ionizing radiations Risks associated with ionizing radiations Risks associated with ionizing radiations. Oxford: Pergamon Press; 1991b;22 (1).

Assessment of Entrance Skin Dose and Effective Dose of Some Routine X-ray Examinations Using Calculation Technique.

Birtch R, Maeshall M: Computation of bremsstrahlung x-ray spectra measured with Ge(Li) detector and comparison spectra measured with Ge(Li) detector. Phs Med Biol 1979;24:505-517.

Bushong SC: Radiographic Science for Technologists: Physics, Radiographic Science for Technologists: Physics, Biology, and Protection, Biology, and Protection, 5th Edition. St. Louis, MO: Mosby-Year Book, 1993.

Christodoulou EG, Goodsitt MM, Chan HP. Phototimer setup for CR imaging. Med Phys 2000;27:2653-8.

Cohen BL (2002) Cancer risk from low level radiation. AJR179:1137–1143.

Curry TS, Dowdey JE, Murry RC: Christensen's Introduction to the Christensen's Introduction to the physics of Diagnostic Radiology physics of Diagnostic Radiology. 3rd ed. Lea & Febiger, Philadelphia, PA, 1984.

D.A. Saia, MA, RT(R) (M) Director, Radiography Program Stamford Hospital Stamford, Connecticut, ed 5, 2009.

Digital Radiography and PACS - Revised Reprint, 1e Revised Edition by Christi Carter MSRS RT(R) (Author), Beth Veale BSRS MEd RT(R)(QM)

(Author).

EC McCullough and JR Cameron: Exposure rates from diagnostic X-ray units ray units, Br J Radiol 1970 43: 448-449.

Egbi - Pediatric radiography entrance doses for some routine procedures in three hospitals within eastern Nigeria, 2008.

European Committee, EC. (1996). European guidelines on quality criteria for diagnostic radiographic images. EUR 16260EN National Radiologic Protection Board. (2000).

Geleijns J, Broers JJ, Chandie MP et al: A comparison of patient dose for examinations of the upper gastrointestinal tract at 11 conventional and digital X conventional and digital X-ray units in the Netherlands. Br J Radiol 1998; 71: 7453.

H. Osman, A. Elzaki, A. Abd Elgyoum, E. Abd Elrahim. (2014) evaluation of radiation entrance skin dose for pediatrics chest x-ray examinations in Taif ,wulfenia journal vol 21, no. 1,60-67.

Hendee WR, Ritenour ER: Medical Imaging Physics, Medical Imaging Physics, Medical Imaging Physics, 3rd Edition. St. Louis, MO: Mosby Year Book, 1992.

Huda W, Slone RM, Belden CJ, Williams JL, Cumming WA, Palmer CK.

Mottle on computed radiographs of the chest in pediatric patients. Radiology 1996;199:249-52.

Hufton AP, Doyle SM, Carty HML. Digital radiography in paediatrics: radiation dose considerations and magnitude of possible dose reduction. Br J Radiol 1998;71:186-99.

ICRP Publication 73, Radiological protection and safety in medicine, Ann, ICRP 26(2) 1996.

International Atomic Agency: International basic safety standards for protection against ionizing radiation and for safety of radiation sources. IAEA Safety Series No. 115-1, IAEA, Vienna 1994.

International Atomic Energy Agency. (1996) International basic standards for protection against ionizing radiation and for the safety of radiation source. Vienna: IAEA Safety Series.

International Commission on Radiological Protection, ICRP: Recommendations of the ICRP recommendations of the ICRP, ICRP publication 60. Annals of the ICRP. Pergamon Oxford. 1991.

Introduction to medical imaging and PACS edition 6. 2009.

IR Edmonds: Calculation of patient skin dose from diagnostic X-ray procedures, Br J Radiol 1984 57: 733-734.

Merrill's atlas of radiographic positions and radiologic procedures, vols I-III. 10th ed. St. Louis, MO: Mosby; 2003.

Montgomery A, Martin J: A study of the application of pediatric reference levels. Br J Radiol 2000; 73: 1083-90.

National protocol for patient dose measurements in diagnostic radiology. Chilton Didcot, UK: NRPB. Report of the working party of the Institute of Physics Science in Medicine

Ng KH, Rassiah P, Wang HB, Hambali AS, Muthuvellu P, Lee HP: Doses to patients in routine X-ray examinations in Malaysia Br J Radiol .1998; 71: 654-60.

Parry, R. A., Glaze, S. A., & Archer, B. R.. (1998). The AAPM/RSNA physics tutorial for residents typical patient radiation doses in RSNA scientific assembly.

PC Shrimpton: Calculation of patient skin dose from diagnostic X-ray procedures, Br J Radiol 1985 58: 483-485.

Radiological protection and safety in medicine Radiological protection and safety in medicine. ICRP publication 73. Annals of the ICRP. Oxford: Pergamon Press; 1996b;26 (2).

Strauss KJ, Poznauskis L. Practical applications of CR in pediatric imaging. App Radiol 2005;June(suppl):S12-8.

Suliman, I.I., Abbas, N. and Habbani, F.I. (2007) Entrance Surface Doses to Patients Undergoing Selected Diagnostic X-Ray Examinations in Sudan. Radiation Protection Dosimetry, 123, 209-214. <http://dx.doi.org/10.1093/rpd/nc1137>.

Tung CJ, Tsai HY: Evaluations of Gonad and Fetal Doses for Diagnostic Radiology, Proc. Natl. Sci. Counc. ROC(B), 1999, 23(3) : 107-113.

Willis CE, Slovis TL. The ALARA concept in pediatric CR and DR: dose reduction in pediatric radiographic exams—a white paper conference executive summary. Pediatric Radiol 2004;34(Suppl. 3): S162–4.

Evaluation of Entrance Skin Radiation Exposure Dose for Pediatrics Examined by Digital Radiography at Asser Central Hospital-KSA

Sami Nasreldein Abdelwally Eljak¹, Caroline Edward Ayad^{2*}, Elsafi Ahmed Abdalla²

¹Radiology Department, Asser Central Hospital, Saudi Arabia, Saudi

²College of Medical Radiological Science, Sudan University of Science and Technology, Khartoum, Sudan

Email: [*carolineayad@yahoo.com](mailto:carolineayad@yahoo.com)

Received 27 May 2015; accepted 19 July 2015; published 23 July 2015

Copyright © 2015 by authors and Scientific Research Publishing Inc.

This work is licensed under the Creative Commons Attribution International License (CC BY).

<http://creativecommons.org/licenses/by/4.0/>



Open Access

Abstract

Assessment of entrance skin doses for patients in Digital radiography examinations should be made as a means for the optimization of the radiation protection of the patients. We measured the entrance skin dose (ESD) received by 50 peditrics undergoing 12 types of diagnostic X-ray examination at Radiology Department of Asser Central Hospital-KSA. The entrance skin dose ESD was determined via measurements parameters: focus to skin distance (FSD), tube current (mAs) and tube voltage (kV) in arithmetical equation. The mean \pm SD for ESDs were found to be 0.16 ± 0.03 , 0.21 ± 0.01 , 0.63 ± 0.26 , 0.55 ± 0.09 , 0.15 ± 0.05 , 0.27 ± 0.06 , 0.41 ± 0.19 , 0.46 ± 0.18 , 0.46 ± 0.12 , 0.20 ± 0.02 , 0.39 ± 0.01 , 0.29 ± 0.03 , for PA chest, foot, AP pelvis, PA skull, PA hand, AP arm, ankle, AP shoulder, abdomen, forearm, AP femur, AP elbow consequently. Our study is considered as an attempt to evaluate the ESDs received by digital radiographic x-ray machine for children aged between 2 - 15 years old, taking in our considerations number of other variables. The mean ESD values obtained are found to be within the standard reference. The data obtained may add to the available information in national records for general use. It may provide guidance on where efforts on dose reduction will need to be directed to fulfill the requirements of the optimization process and serve as a reference for future researches.

Keywords

Entrance Skin Dose, Pediatrics, Digital Radiography

*Corresponding author.

1. Introduction

In radiology field dose assessment should be made to enhance the optimization of the radiation protection of the patients and to deliver minimum dose to the examinations. Dose measurements are necessary for the fulfillment of the international guidelines and regulations [1].

It is known that children diagnostic radiological examinations have higher risk when compared to the ones carried out for adults. Young individuals have longer life expectancy and their developing tissues are more radiosensitive. The relative risk of harmful effect after radiation exposure during the first 10 years of life is 3 to 4 times if compared to an exposure for 30 or 40 years old [2]. Children have a risk of developing a radiation-induced cancer, because of their greater cell proliferation rate and long life span expectancy [3].

Entrance surface Dose (ESD) is a measure of the radiation dose absorbed by the skin where the X-ray beam enters the patient [1], it have been used to report patient doses, and this has been studied for pediatric patients all over the world [4]. In Saudi Arabia few studies have been carried out in patient radiation concerns, especially with regards to children, moreover work was concerned with calculation of the ESD for pediatric patients undergoing X-ray examinations in a pediatric hospital took place in Taif hospital [5].

Our aim in this study was to measure the entrance skin dose (ESD) for pediatrics undergoing diagnostic X-ray examinations in four hospitals (Asser Central Hospital-Saudi Arabia). To the best of our knowledge, no study was done in the open literature regarding that issues.

2. Materials and Methods

2.1. Selection and Description of Participants

This prospective study was performed in the period of August 2013 to September 2014. Patients were examined at the radiology department of Asser Central Hospital-Saudi Arabia. Prior to patients examined, a formal approval was obtained from the Ethics and Scientific Committee of this medical center. Informed consents were obtained from patients.

2.2. Digital Radiography Machine

(AXIOM Aristos FX/FX Plus system—Siemens). Manufactured for GE Health care, Milwaukee, wi By Siemens, S.N: 4927, Model: ALOIC II, Manufactured: February/2013, Location: Kemnath/Germany, Type: 5234954, Filtration: 2.0 mm Al/70 KV, Localizer Lights: 24 v, 150 W.

2.3. Parameters and Measuring ESD

Different radiological examinations including: Foot, AP Pelvis, Skull PA, PA Hand, AP Arm, Ankle, AP Shoulder, Forearm, AP Femur, AP Elbow, were included, these examinations were obtained using fine focus and FFD of 100 cm. Chest PA and Abdomen were obtained by using broad focus and FFD 180 - 100 cm respectively. Patient information including age, gender, weight, BMI, height was considered. The type radiological examination and applied projection as well as the exposure details such as tube voltage (KV), tube current (MAS), organ thickness, focal to skin distance (FSD) were evaluated. Data were collected on patient doses during the period from 2013-2014. The ESD was calculated according to the following equation which was applied by (Tung and Tasi; 1999) [6].

$$ESD = c \left(\frac{KVp}{FSD} \right)^2 \left(\frac{mAs}{mm.Al} \right) \quad (1)$$

where:

ESD stands for Entrance skin dose, c = constant = 0.2775, Kvp = Applied Tube potential, mAs = Tube current multiplied by exposure time, FSD = Focus to skin distance, Al = Aluminum Filtration.

2.4. Statistical Analyses

Data were presented as mean \pm SD in a form of comparison tables. Statistical analysis was performed using the standard Statistical Package for the Social Sciences (SPSS Inc., Chicago, IL, USA) version 16. ANOVA and person correlation, Independent t-test were used. Correlation is significant at the $p < 0.05$.

3. Results and Discussions

The mean and \pm SD values of all the pediatrics examined in the study were presented in (Table 1). Study population comprised 50 pediatric patients (26 males and 24 females). Pediatric ages ranged from 2 to 15 years; with a mean age of (7.19 ± 3.10) years, weight ranged from 21 to 51 Kg; with a mean value of (22.31 ± 7.86) years, mean height of (117.4 ± 17.36) years, height ranged from 86 to 140 cm; the smallest BMI of the population was 13.2 and the largest value was 26.4.

The mean and \pm SD of the Digital Radiography X-ray machine parameters were presented in (Table 2). The maximum Kv was found to be 74, mAs of 10, organ thickness 16 cm, Focus to Skin Distance (FSD) of 168.5 and the measured ESD was of 0.92.

Mean and standard deviation for ESDs in mGy for the radiological examinations were compared with other authors, and were presented in (Table 3), The maximum ESD was found in the AP pelvis (0.63 ± 0.26) and the minimum dose was found in PA hand (0.15 ± 0.05). It was found that the dose level received by the digital radiography machine in our hospital were lower than other studies levels [7], [8] with significant difference at $p < 0.000$ in respected to different type of X-ray examinations. The justification may be due to the fact that the digital X-ray machine was manufactured with high engineering technology and gave low doses because of the cathode cup is optimized for use in a line-focus, planar anode tube and has a slot in which the emitter is situated. Table 3 showed that the ESD (mGy) for the PA chest was close to that reported by the (NRPB, 2000) [8] mGy, but lower than the value of European Commission [7] by 0.14 mGy. The ESD (mGy) for the AP pelvis was lower than the value that reported by European Commission [7] by 3.7 mGy may be due to the patients thickness under study. The ESD (mGy) for abdomen half than value recorded by the European Commission [7] and close to that values reported by National Radiological Protection Board [8] and (IAEA, 1996) [9].

Similar examinations carried out in Sudan at four hospitals, eight X-ray units, their hospital mean ESDs estimated range from 0.17 to 0.27 mGy for chest AP, 1.04 - 2.26 mGy for Skull AP/PA [10].

The radiological technique including AP, Dorsi planter, lateral and oblique projections have no impact on the ESDs measures it ranged between 0.15 - 0.33 mGy Dorsi planters and oblique have less ESD than other projections (Table 4).

The maximum pediatric age class was found at ages between 6 - 9 years, they constituting 23 pediatric patients. The maximum ESD received was for pediatric of ages of 10 and more; however there is no significant relation between age classes and ESD (Table 5).

Table 1. Pediatrics demographic data.

	Age/years	Weight/Kg	BMI	Height/cm
Mean	7.19	22.31	15.76	117.44
Median	7.25	23.00	15.20	124.00
Std. Deviation	± 3.10	± 7.86	± 2.17	± 17.36
Minimum	2.0	12.00	13.20	86.00
Maximum	15.0	51.00	26.40	140.00

Table 2. Mean and standard deviation of the digital radiography X-ray machine.

	Tube Voltage (Kv)	Tube Current (mAs)	Organ Thickness	Focus to Skin Distance (FSD)	Entrance Skin Dose (ESD)
Mean	63.76	5.32	7.01	103.59	0.33
Median	65.00	5.50	5.00	96.00	0.29
Std. Deviation	± 5.98	± 1.94	± 4.19	± 24.69	± 0.18
Minimum	48.00	2.00	2.00	85.00	0.11
Maximum	74.00	10.00	16.00	168.50	0.92

Table 3. Mean and standard deviation for ESDs in mGy for the radiological examinations were compared with other authors.

	Entrance Skin Dose (ESD)					Other Authors	
	N	Mean	Minimum	Maximum	<i>p</i> -Value	EC, 1996 mGy [7]	NRPB, 2000 mGy [8]
Chest PA	7	0.16 ± 0.03	0.11	0.20	0.000	0.3	0.2
Foot	2	0.21 ± 0.01	0.21	0.21		-	-
AP Pelvis	3	0.63 ± 0.26	0.41	0.92		10	4
Skull PA	6	0.55 ± 0.09	0.42	0.69		5	3
PA Hand	6	0.15 ± 0.05	0.12	0.25		-	-
AP Arm	5	0.27 ± 0.06	0.17	0.32		-	-
Ankle	2	0.41 ± 0.19	0.27	0.55		-	-
AP Shoulder	3	0.46 ± 0.18	0.29	0.64		-	-
Abdomen	6	0.46 ± 0.12	0.29	0.62		10	-
Forearm	4	0.20 ± 0.02	0.19	0.22		-	-
AP Femur	2	0.39 ± 0.01	0.39	0.41		-	-
AP Elbow	4	0.29 ± 0.03	0.28	0.34		-	-
Total	50	0.33 ± 0.18	0.11	0.92			-

Table 4. Mean and standard deviation for ESDs in mGy according to the radiological technique.

	Entrance Skin Dose (ESD)					<i>p</i> -Value
	N	Mean	Std. Deviation	Minimum	Maximum	
AP	30	0.37	±0.20	0.113	0.919	0.105
Dorsi Planter	4	0.15	±0.04	0.120	0.214	
Lateral	15	0.33	±0.13	0.136	0.547	
Oblique	1	0.16	±0.0	0.163	0.163	
Total	50	0.33	±0.18	0.113	0.919	

Table 5. Mean and standard deviation for ESDs in mGy according to the pediatrics ages.

Age/Years	Entrance Skin Dose (ESD)					<i>p</i> -Value
	N	Mean	Std. Deviation	Minimum	Maximum	
2 - 5 y	16	0.29	±0.17	0.120	0.693	0.344
6 - 9 y	23	0.34	±0.17	0.113	0.630	
≥10 y	11	0.39	±0.23	0.157	0.919	
Total	50	0.33	±0.18	0.113	0.919	

Gender and body characteristics including weight, height, BMI, had no impact on the ESDs, however the organ thickness had a significant relation with ESD at $p < 0.000$ (Table 6 and Table 7). Correlations between Entrance Skin Dose (ESD) and exposure parameters showed significant relation (Table 8). Many authors stated that the absorbed dose in skin is directly proportional to tube current; the length of exposure, and the square of peak kilovoltage [11]. Our justification was that the digital imaging X-ray machine may allow for use of a lower tube current or a shorter exposure, thus reducing the dose to the patient as mentioned previously [11] and where the image quality controlled automatically because the using of automatic exposure control as well as the presence of aluminum filter of 2.0 mm.

Table 6. Mean and standard deviation for ESDs in mGy according to gender.

Gender	N	Entrance Skin Dose (ESD)				p-Value
		Mean	Std. Deviation	Minimum	Maximum	
Male	26	0.32	±0.19	0.122	0.693	0.549
Female	24	0.35	±0.18	0.113	0.919	
Total	50	0.33	±0.18	0.113	0.919	

Table 7. Correlation between the Entrance Skin Dose (ESD) and the pediatrics body characteristics.

Correlations between the Entrance Skin Dose (ESD) and the Pediatrics Body Characteristics		
Weight/Kg	Pearson Correlation	0.064
	Sig. (2-tailed)	0.657
	N	50
BMI	Pearson Correlation	-0.175
	Sig. (2-tailed)	0.224
	N	50
Height	Pearson Correlation	0.189
	Sig. (2-tailed)	0.189
	N	50
Organ Thickness	Pearson Correlation	0.364**
	Sig. (2-tailed)	0.009
	N	50

*Correlation is significant at the 0.05 level (2-tailed). **Correlation is significant at the 0.01 level (2-tailed).

Table 8. Correlation between the Entrance Skin Dose (ESD) and exposure parameters

Correlations between Entrance Skin Dose (ESD) and Exposure Parameters		
Tube Voltage (KV)	Pearson Correlation	0.351*
	Sig. (2-tailed)	0.013
Tube Current (MAs)	Pearson Correlation	0.709**
	Sig. (2-tailed)	0.000
Focus to Skin Distance (FSD)	Pearson Correlation	-0.491**
	Sig. (2-tailed)	0.000
Total Number	N	50

*Correlation is significant at the 0.05 level (2-tailed). **Correlation is significant at the 0.01 level (2-tailed).

However, the risk from radiation exposure of the patients must be balanced versus the diagnostic benefit. Many departments do not use recommended radiographic parameters for children using digital radiography, furthermore, wide variations in the applications of the radiographic techniques, equipment performance at different hospitals over the world.

4. Conclusion

Our study in Saudi Arabia at Asser Central Hospital-KSA is considered as an attempt to evaluate the ESDs re-

ceived by digital radiographic X-ray machine for children aged between 2 - 15 years old, taking in our considerations number of other variables. For all the examinations studied in the hospital, the mean ESD values obtained are found to be within the standard reference values of doses. The data obtained may add to the available information in national records for general use. It will provide guidance on where efforts on dose reduction will need to be directed to fulfill the requirements of the optimization process and serve as a reference for future researches and in pediatrics of ages less than two years old.

Acknowledgements

Thanks for Asser Central Hospital-KSA, and Sudan University of Science and Technology, College of Medical Radiological Science, Khartoum, Sudan.

References

- [1] Taha, M.T., Al-Ghorabie, F.H., Kutbi, R.A. and Saib, W.K. (2015) Assessment of Entrance Skin Doses for Patients Undergoing Diagnostic X-Ray Examinations in King Abdullah Medical City, Makkah, KSA. *Journal of Radiation Research and Applied Science*, **8**, 100-103.
- [2] United Nations Scientific Committee on Effects of Atomic Radiation. Sources and Effects of Ionizing Radiation. UNSCEAR 2000 Vol. 1, Report to the General Assembly. New York, 2000.
- [3] Persliden, J., Helmorot, E., Hjort, P. and Resjo, M. (2004) Dose and Image Quality in Comparison of Analogue and Digital Techniques in Paediatric Urology Examinations. *European Radiology*, **14**, 638-644. <http://dx.doi.org/10.1007/s00330-003-2144-9>
- [4] Osman, H., Elzaki, A., Abd Elgyoum, A. and Abd Elrahim, E. (2014) Evaluation of Radiation Entrance Skin Dose for Pediatrics Chest X-Ray Examinations in Taif. *Wulfenia Journal*, **21**, 60-67.
- [5] Osman, H. (2013) Pediatric Radiation Dose from Routine X-Ray Examination Hospital Based Study, Taif Pediatric Hospital. *Scholars Journal of Applied Medical Sciences*, **5**, 511-515.
- [6] Tung, C.J. and Tsai, H.Y. (1999) Evaluations of Gonad and Fetal Doses for Diagnostic Radiology. *Proceedings of the National Science Council, Republic of China. Part B, Life sciences*, **23**, 107-113.
- [7] European Committee (EC) (1996) European Guidelines on Quality Criteria for Diagnostic Radiographic Images. EUR 16260EN.
- [8] National Radiologic Protection Board (2000) National Protocol for Patient Dose Measurements in Diagnostic Radiology. Report of the Working Party of the Institute of Physics Science in Medicine, NRPB, Chilton Didcot.
- [9] International Atomic Energy Agency (1996) International Basic Standards for Protection against Ionizing Radiation and for the Safety of Radiation Source. IAEA Safety Series, Vienna.
- [10] Suliman, I.I., Abbas, N. and Habbani, F.I. (2007) Entrance Surface Doses to Patients Undergoing Selected Diagnostic X-Ray Examinations in Sudan. *Radiation Protection Dosimetry*, **123**, 209-214. <http://dx.doi.org/10.1093/rpd/nci137>
- [11] Parry, R.A., Glaze, S.A. and Archer, B.R. (1999) The AAPM/RSNA Physics Tutorial for Residents Typical Patient Radiation Doses in Diagnostic Radiology. *Radiographics*, **19**, 1289-302.

CHAPTER ONE

CHAPTER TWO

CHAPTER THREE

CHAPTER FOUR

CHAPTER FIVE

REFERENCES

PUBLICATION